SCALABLE PRODUCTION OF GRAPHENE OXIDE AND QUANTUM DOTS BY CHEMICAL ROUTE AND THEIR COMPARATIVE ANALYSIS.

A DISSERTATION

SUBMITTED IN PARTIAL FULFILLMENT OF THE REQUIREMENTS
FOR THE AWARD OF DEGREE
OF

MASTER OF TECHNOLOGY

IN

NANOSCIENCE AND TECHNOLOGY

Submitted By

SUPRIYA BISWAS

(Roll No. 2K17/NST/04)

Under the supervision of

DR. M. S. MEHATA

(ASSISTANT PROFESSOR)

DEPARTMENT OF APPLIED PHYSICS

Delhi Technological University

(Formerly Delhi College of Engineering)

Bawana Road, Delhi-110042

JUNE,2019

DELHI TECHNOLOGICAL UNIVERSITY

(Formerly Delhi College of Engineering)

Bawana Road, Delhi-110042

CANDIDATE'S DECLARATION

I, Supriya Biswas, Roll No. 2K17/NST/04 of M.Tech. Nanoscience and Technology, hereby declare that the project Dissertation titled **"Scalable production of grapheme oxide and quantum dots by chemical route and their comparative analysis"** which is submitted by me to the Department of Applied Physics, Delhi Technological University, Delhi in partial fulfillment of the requirement for the award of the degree of Master of technology, is original and not copied from any source without proper citation. This work has not previously formed the basis for the award of any Degree, Diploma Associate ship, Fellowship or other similar title or recognition.

Place, Delhi, INDIA **Supriya Biswas**

Date:

DELHI TECHNOLOGICAL UNIVERSITY

(Formerly Delhi College of Engineering)

Bawana Road, Delhi-110042

CERTIFICATE

I hereby certify that the Project Dissertation titled **"Scalable production of graphene oxide and quantum dots by chemical route and their comparative analysis"** by **Supriya Biswas**, Roll No. **2K17/NST/04**, Department of Applied Physics, Delhi in partial fulfillment of the requirement for the award of the degree of Master of Technology, is a record of the project work carried out by the student under my supervision. To the best of my knowledge, this work has not been submitted in part or full for any Degree or Diploma to this University or elsewhere.

Place: Delhi **Dr. M.S. Mehata**

Date: **Supervisor**

ACKNOWLEDGEMENT

With great pleasure and respect, I express my heartfelt gratitude to my supervisor **Dr. M. S. Mehata, Assistant Professor, Applied Physics, Delhi Technological University** for his constant support, motivation and patience during my entire M.Tech dissertation. I'm very thankful to him for providing me with such excellent in-house lab facilities due to which I can complete my project.

I would also like to express my deepest regard to my parents for always supporting and standing by me in every decision of my life. Without their sacrifices and love I wouldn't had made this far. A special mention to my elder sister Ria Biswas and brother-in-law Rohitashva Shukla for always encouraging and showing me the right direction.

I'm very obliged to the **Head of Department Prof. Rinku Sharma** and all the faculty members of the Applied Physics department for all the support and guidance. I would like to convey a special thank you to all the Phd Scholars of the Laser spectroscopy lab especially Mrityunjay Singh and Prateek Sharma for all the guidance and help during my dissertation.

Last but not the least I'm really thankful to my friends Priti Rani, Sachin kharb and Jyotsna Singh for being there always through all the thick and thin. You guys made the entire hustle so much worthy.

TABLE OF CONTENTS

LIST OF FIGURES

LIST OF TABLES

LIST OF EQUATIONS

ABSTRACT

Graphene, the wonder material is known for it's excellent properties which are due to it's unique geometry, high mechanical and thermal strength and electrical conductivities. It has great electrical stability and impermeability. Among the various techniques that are available for its synthesis, modified hummers method is widely used for the scalable production of graphene oxide (GO). Recently, GO has attracted massive attention from the researchers due to it's unique properties like though it is an insulator it shows fluorescence behaviour due to the presence of oxygenated functional groups along it's edges and basal planes. The FT-IR spectrum of GO shows the presence of many functional groups which are confined into the sp^2 and sp^3 sites present on it's structure. Since, it is a monolayer sheet of graphite it's XRD peak clearly indicates how it doubles the inter-layer separation between the stacks. To improve it's conductivity we perform the oxidative cutting of GO sheets by strong acids to synthesize graphene quantum dots (GQDs). These GQDs are readily used for optoelectronic applications. The as prepared GQDs show excellent conductivity and reduction in bandgap. On contrary to GO the fluorescence in GQDs are due to defects and trap sites. Due to quantum confinement effect and reduction of size the GQDs are luminescent and they show green colour when exposed to ultra-violet light. Thus, though both GO and GQDs are fluorescent the emission spectra of GO is independent of excitation wavelengths but the fluorescence of GQDs depend not only on the excitation wavelengths but also on the pH value of the solution. Thus, in this thesis, we have synthesized both GO and GQDs by using chemical route and have evaluated their similarities and differences by various characterizing methods.

Chapter 1 : Introduction & History

1.1 Background

Canadian physicist Philip Russell Wallace [1] was the first who introduced the concept of graphene in 1947. He studied graphite along different lattice directions and estimated it's electrical conductivity by theoretical calculations. In his study, the conductivity of graphite was found to be 100 times greater along the graphene plane compared to other directions. Since his entire study was focussed on the properties of graphite rather than graphene he never used the term "graphene". Instead, he just referred to it as "single hexagonal layer". Little did he knew that this '"single hexagonal layer" is the wonder material which will revolutionized the coming age technology and will even lead to nobel prize for two gentlemen in the coming half century.

1960s was the first time when attempts were made to synthesize graphene with very little knowledge about it's properties and methods to produce it. Karu and Beer [2] used a chemical vapor deposition technique in their experiment where a nickel substrate was exposed to hydrocarbon precursor gas such as methane at a controlled temperature. It was observed that the growth rate of carbon on the substrate was decreasing dramatically compared to the growth of carbon in vertical direction. Compared to single layer graphene film the magnitude of exposure time for the double- layer graphene film is more such that in the order of one or two. Thus by altering the exposure time they were able to control the thickness of the graphene film produced. Carbon atom segregation from carbon doped substrate to the surface while undergoing thermal annealing is another method which was used for the growth of carbon on substrate [3]. The annealing temperature can control the number of segregated carbon to the surface thereby it can control the growth rate. Though it was proved successful to grow single layer graphene from both chemical vapor deposition (CVD) and C-atom segregation methods, the challenging part was to differentiate the grown graphene layers from the catalytic substrate without hindering the structural integrity. Thus, the graphene adhered on the substrate suffer from varied electronic properties due to disruption by the substrate.

2004 was the year when Andre Geim and Novoselov [4] were finally successful in isolating single layer of graphene. The story of this discovery is rather fascinating. The love for

science made these two scientists to hold “Friday night experiments” where they would meet and perform simple experiments just for fun so that their curiousity, interest and love for science can never die away. In one of these parties, Geim and Novoselov found that they can pull apart a piece of graphite into two thinner pieces using a scotch tape. An intriguing idea hit them that if they keep pulling apart the thinner pieces, eventually they would reach a point where they would have pieces of single graphene layers. They put that idea into action and made it work. Today, this primitive way of obtaining single layer graphene, so called a “scotch tape” method, was publicly displayed in the Nobel prize museum in memory of this discovery. Looking back to Geim and Novoselov’s “Friday night experiments”, it is inspiring to know that raw enthusiasm and curiosity are still pushing science forward, even in such an advanced world.

1.2 Graphene

Graphene is a monolayer precious stone of carbon particles, normally shed from graphite. It has a honeycomb hexagonal cross section created by sp^2 hybridized bonds. The rhombic unit cell of single layer graphene contains two carbon particles [fig 1]. The C-C separation is 0.142 nm. The graphene is anything but an ideal 2D plane, however contains swells around 1 nm in size.

Structure

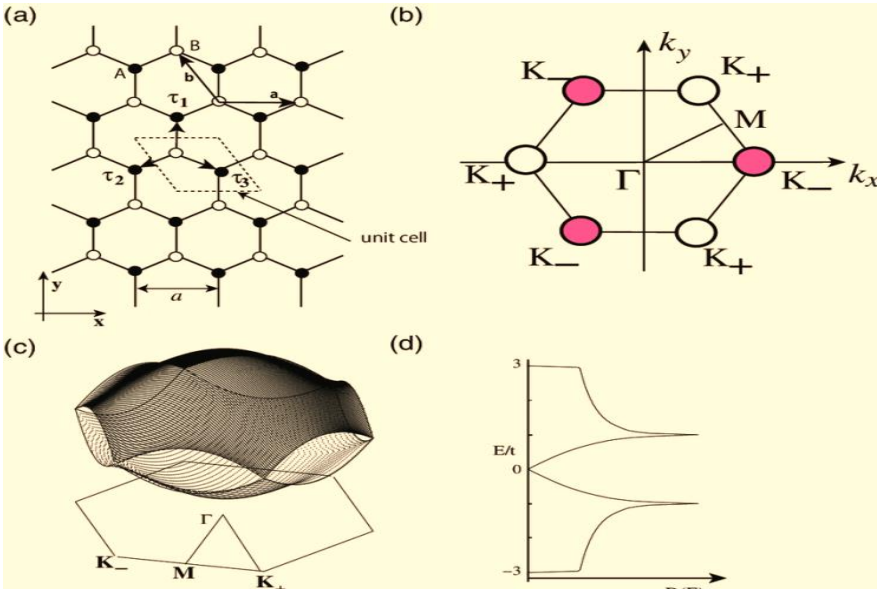

Fig 1:(a) Graphene sheet in lattice space, where the dark (white) circles mean sub lattice site; a_n is the cross section consistent and a = (a, 0) and b = (−a/2, √ 3a/2) are the space vectors. Here τ_1 = (0, a/√

3), $\tau_2 = (-a/2, -a/2\sqrt{3})$ and $\tau_3 = (a/2, -a/2\sqrt{3})$. (b) First Brillouin zone of graphene $K+ = 2\pi/a(1/3, 1/\sqrt{3})$, $K- = 2\pi/a(2/3, 0)$,$\Gamma = (0, 0)$.(c) The π-band structure and (d) the thickness conditions of a graphene sheet. The valence and conduction groups reach at the dirac point K ±1 [5].

Electrical Properties

Graphene has been found as a zero-gap semiconductor [6]. As appeared in Figure 1(c) and (d), the valence groups meet the conduction groups at Dirac focuses and Dirac focuses situate on the six corners of the Brillouin zone in force space [6]. There are two non-identical arrangements of Dirac focuses marked K and K'[fig 2 (a) and (b)].The conduction and valence groups cross at focuses K and K'— the two non-equal corners of the zone, otherwise called the Dirac focuses; Because of the straight scattering close to the Dirac focuses, the charge transporters (openings and electrons) can change to one another without energy utilization [6]. These accuse transporters of low vitality can be depicted as massless Dirac fermions [6]. By changing the connected electric field, the particular bearer thickness can be changed also. Another preferred position from the nearness of Dirac focuses is the electronic ballistic transport of charge bearers in graphene [6]. Charge transporters in graphene carry on like relativistic particles with a powerful speed of light given by the Fermi velocity [5]. The ballistic mean free way of graphene charge bearers can be 0.3μm [7]. This conduct draws in much research consideration and ends up a standout amongst the most captivating properties of graphene.

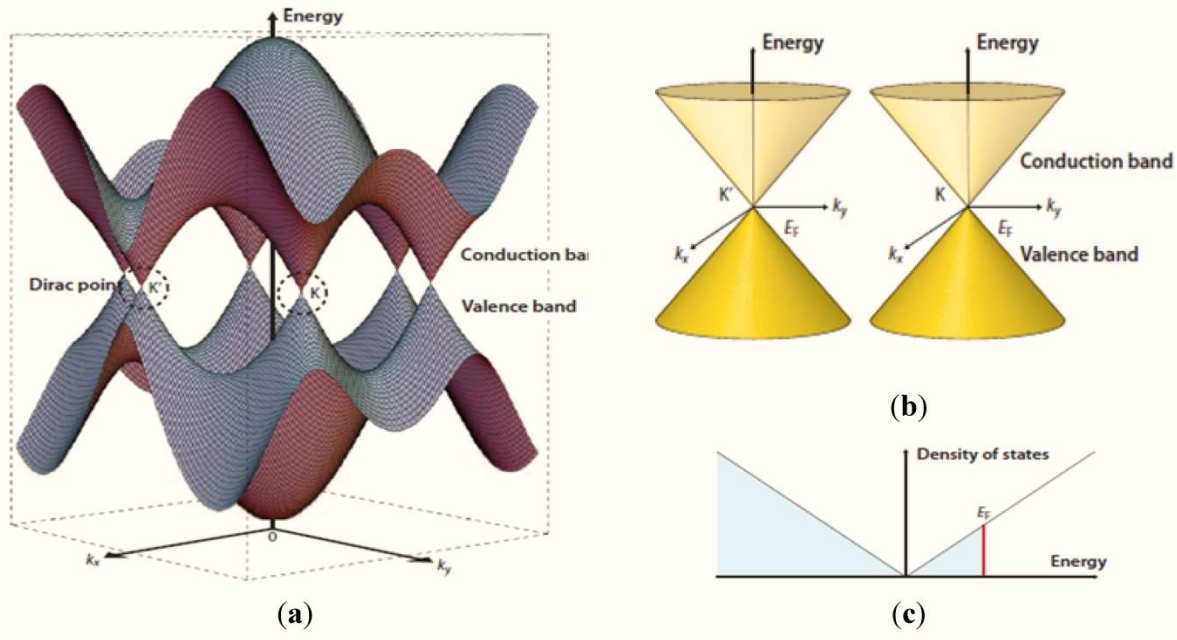

Fig 2:(a) Energy groups close to the Fermi level in graphene. The first Brillouin zone of graphene is represented in the even plane and marked with certain focal points. (b) Conic energy groups in the region of the K and K' focuses; (c) Density of states close to the Fermi level with Fermi energy E_F [7].

Synthesis strategy

The principal single layer graphene was removed from exceedingly situated pyrolytic graphite by Andre Geim and Kostya Novoselov [4] utilizing the scotch tape. As of not long ago, there is no procedure built up that can make graphene test with such high transporter portability and low thickness of deformities [9]. In any case, mechanical peeling is constrained underway scale and tedious. This detriment restricts the application to major research of graphene. After over 10 years' advancement, for the present modern generation of graphene, there are two noteworthy blend courses: base up epitaxial development and top-down shedding [10]. The base up epitaxial development approach includes the immediate union of graphene materials from the carbon sources [10]. A common strategy, for instance, is the synthetic vapor affidavit (CVD). CVD is normally used to develop huge scale, single or multi-layer graphene sheets on metal substrates with low deformities thickness [10, 11]. In an unexpected way, the top-down methodologies, for example, decrease of graphene oxide (GO) take points of interest of high return, simplicity of execution, and arrangement based procedure capacity [10, 12]. Specifically, the minimal effort and large scale manufacturing of diminished graphene oxide sheets has been acknowledged [10, 13]. The Fig 3 abridges the advantages and disadvantages of normal creation techniques for graphene.

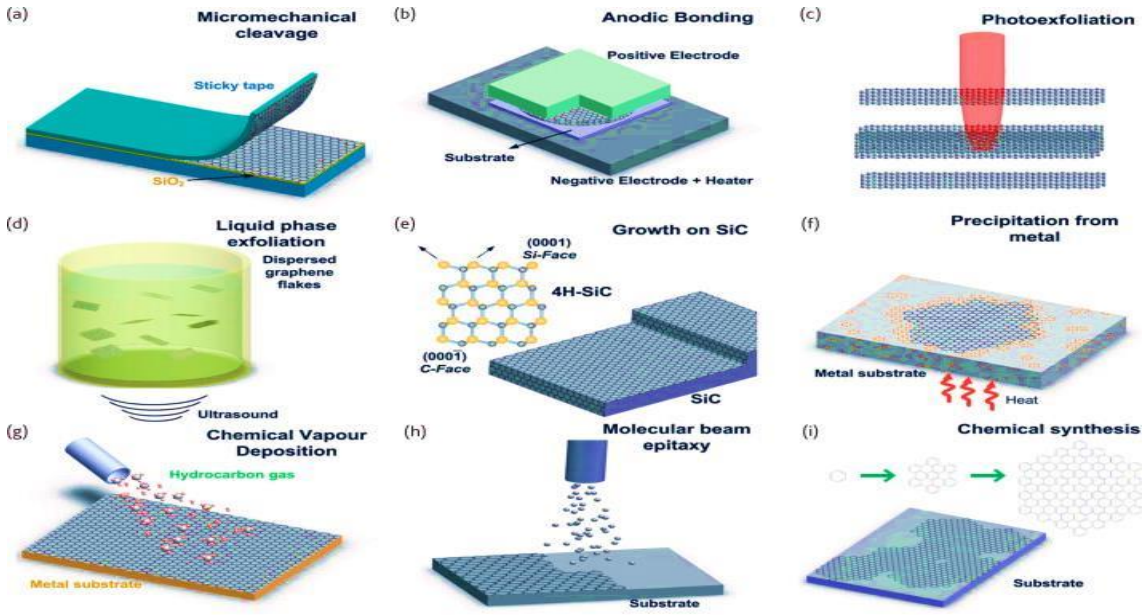

Fig 3: Comparison of the different graphene production methods.(a)Micromechanical cleavage.(b) Anodic Bonding.(c)Photo exfoliation.(d) Liquid Phase Epitaxy.(e)Growth on SiC.(f)Precipitation from metal.(g)Chemical vapour deposition.(h)Molecular beam epitaxy.(i)Chemical Synthesis [8].

Among these strategies, decrease of graphene oxide (GO) was believed to be a standout amongst the most complex techniques to accomplish the enormous scale and minimal effort creation of graphene [12 and fig 3]. GO as a profoundly oxidized sheet is incorporated from solid oxidation of flawless graphite pursued by mechanical shedding, for example, ultra-sonication in fluid media or simply blending [11, 13]. The π system of the graphene adds to the conductive normal for graphene, so the GO must be diminished to recoup its π bond [12]. The GO are generally decreased by electrochemical, warm and substance forms [12]. The items don't have a superb in view of the nearness of extraneous imperfections (oxygen gatherings) and characteristic deformities (edges and disfigurements), yet this strategy permits the creation with high return and moderately low expenses. In this way, oxidation of graphite, mechanical peeling and decrease of GO are the mainstream strategies to deliver business graphene. The most prevalent techniques detailed as of late [13-18] are concoction vapor affidavit (CVD) or plasma upgraded compound vapor testimony (PECVD) which can deliver enormous scale and moderate quality graphene films.

1.3 Graphene Oxide

In spite of the fact that the scotch tape technique provided a total new guidance to the investigation of graphene however despite everything it stayed unreasonable for all intents and purposes when the large scale manufacturing of single layer graphene was considered. This lead to the improvement of a helpful strategy which is known as adjusted hummers technique [21-24]. It was route back in the mid 1958, when Hummers strategy was made remembering the security and proficiency for delivering graphite oxide [25]. The procedure included the expansion of graphite powder or drops into an answer of potassium permanganate and sulphuric corrosive. After the oxidation methodology, oxygenated utilitarian gatherings, for example, hydroxyl gatherings and epoxide gatherings, was framed on the outside of individual graphite layers. Being hydrophilic in nature these utilitarian gatherings will effectively let water particles to be promptly intercalated between the layers when graphite oxide is scattered in watery medium. Together with ultrasonic medicines this technique will totally shed graphite oxide to shape a steady scattering of single layered

graphene oxide. The as readied graphene oxide will incompletely be changed over once more into monolayer graphene by utilizing compound decrease. So the all-out mix of Hummers technique, ultrasonic peeling and synthetic decrease together known as changed hummers strategy [26].It has been broadly received as a shoddy and effective method for creating huge amounts of single layered graphene. Be that as it may, the thorough oxidation procedure lead to numerous basic harm on graphene created by the changed Hummers strategy. Deformities framed on the graphene plane, in spite of the fact that they regularly expedite undesirable impacts electronic properties, assume a significant job on physicochemical and optical properties of graphene quantum spots.

The one of a kind thermal, structural, electrical, mechanical and optical property of graphene, a two dimensional carbon material has pulled in extraordinary consideration from each circle as of late. By and by, the fundamental strategies for enormous scale assembling of graphene are revolved around the arrangement based concoction redox responses. Experiencing oxidation, the graphite surface ends up open to a great deal of oxygen useful gatherings, which makes graphene oxide (GO) sheets hydrophilic to shape stable liquid colloids. In any case, the rough material graphite gradually loses its conductivity during oxidation strategy as a segment of planar sp^2-hybridized geometry changed to contorted sp^3-hybridized geometry, because of which its astounding electronic properties are lost. Therefore, decrease of GO is absolutely critical to recover its "lost" electrical conductivity for practical applications.

While graphite has confinement only in one dimension and it has freedom of movement in all the three dimensions compared to other carbon based material. It is made up of an humongous compiled of layers of graphene stacked together, graphite oxide(GTO) has different configuration [14].The strong acids and materials which help in its oxidation, oxygenated functionalities are displayed in the graphite structure which increment the structural distances, yet moreover makes the material water seeking [15]. This property makes the GTO to be shed in water using sonication, finally making uni or multi-layer graphene, known as graphene oxide (GO). The essential refinement between graphite oxide and graphene oxide is, as such, the amount of stacks and separation [15]. While GTO is a many layer system in a GO dispersing, a few layers pieces and monolayer chips can be found. One of the upsides of the graphene oxide is its straightforward dispersability in water and other common solvents, similarly as in different systems, in view of the proximity of the oxygen functionalities [15]. This goes about as a huge property when ading the substance

with imaginative or polymer structures when trying to improve their conductive and strengthening properties.

On the other hand, similar to electrical conductivity, graphene oxide is much of the time depicted as an electrical separator, in view of the intrusion of its sp^2 holding networks [16]. In order to recover the honeycomb hexagonal cross segment, and with it the electrical conductivity, the decrease of the GO must be practiced [fig 5 (a) and (b)]. It must be viewed as that once most of the oxygen social occasions are removed, the lessened GO obtained is progressively difficult to dissipate in light of its tendency towards collection. Functionalization of graphene oxide can on an exceptionally essential dimension change graphene oxide's properties [17]. The consequent artificially adjusted graphenes could then end up being impressively progressively flexible for a lot of applications. There are various habits by which graphene oxide can be functionalized, dependent upon the perfect application. Graphene oxide (GO), as one of the source materials for amalgamation of graphene, has been inspected starting late. Not simply the tremendous scale graphene age can be cultivated by decreasing GO easily, yet likewise the GO itself has various potential applications in batteries and clear conductors. A definite GO helper model can empower us to fathom the electronic, mechanical and optoelectronic properties of GO. Accordingly, we can structure new GO composites or intentionally tune the properties of GO reliant on the model. Regardless of the way that there are various preliminary and speculative models, the authentic structure of GO still remains questionable [fig 4 (a) and (b)]. One reason is that these models sort out the oxygen packs physically in a fixed cell inside a limited scale, yet the certified GO may be non-stoichiometric and non-infrequent in the long range.

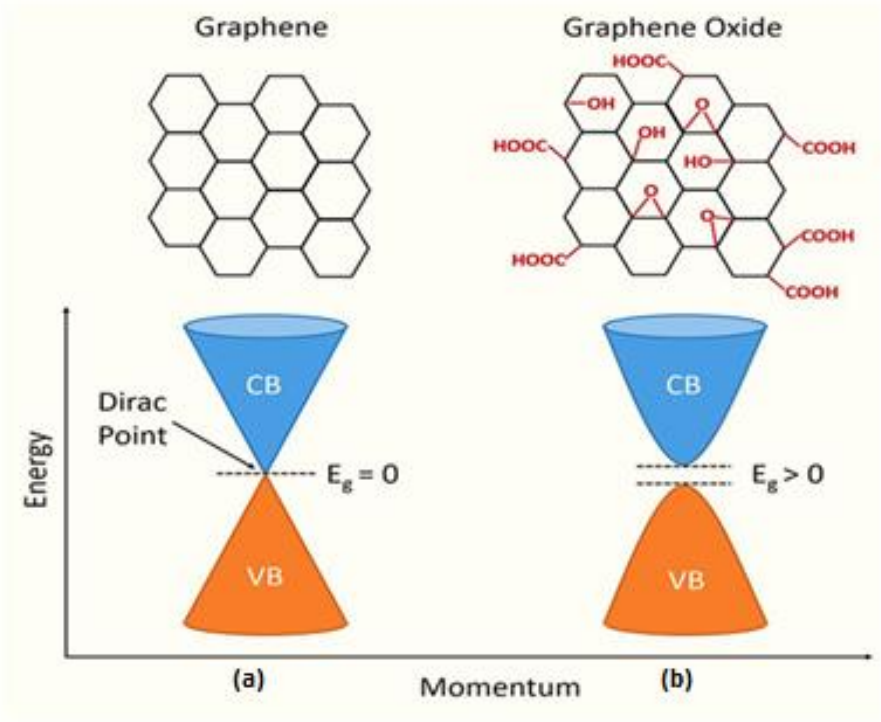

Fig 4: The difference in the structure and energy bandgap of (a) graphene and (b) graphene oxide [9].

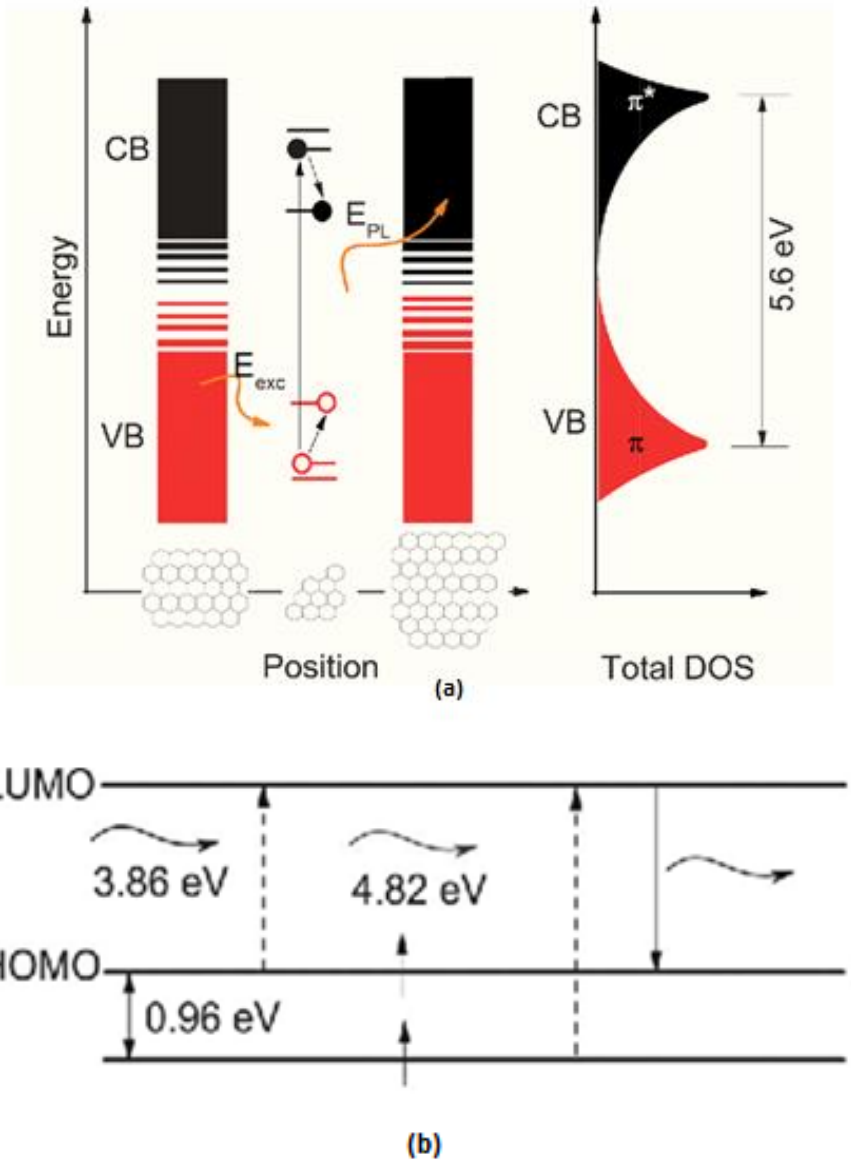

Fig 5: (a) Band edge distribution of GO.(b) The difference between the highest occupied level and the lowest empty level which results in photoluminescence in GO is shown [5].

1.4 Graphene quantum dots (GQDs)

Graphene quantum dabs (GQDs) are artifically similar to graphene oxide, yet are confined graphene pieces with the estimation of a couple to 20 nm. The limited opportunity of development over all the three dimensions grants them a unique optical properties, explicitly, photoluminescence, in view of a quantum constrainment effect [27-28]. In the going with section, the possibility of quantum control will be immediately depicted.

Bohr radius

The Bohr radius can be closed by two significant things. It is possible that it is characterized as a mean separation between a photon and an electron limited in a hydrogen particle at its ground level. It has an estimation of 5.29×10^{-11} m. Here in this proposal we are alluding to Bohr range as the size of eletron-gap sets (prevalently known as excitons) delivered by excitation of electrons by photons. As such it can likewise be alluded as the mean detachment between a photon produced electron and it's relating opening caught in a nanoparticle. The estimation of Bohr radius (αβ) is given as

$$\alpha\beta = \varepsilon\{m/(m^{\circ})\}\alpha^{\circ} \text{ ---------- (1)}$$

Where m speaks to the mass of the molecule, m˚ speaks to the rest mass of the electron, αβ is the Bohr range of the hydrogen particle, and ε is the dielectric consistent of the material. An exciton can uninhibitedly move with no limitation when the size of the molecule is bigger than the de Broglie wavelength or at the end of the day is more noteworthy than twofold its size claim Bohr sweep. Nonetheless if the molecule size diminishes to a dimension when it decreases than twofold of its own Bohr sweep or de Broglie wavelength it's development gets limited in space because of the presentation of quantized vitality levels. This wonder of quantization of vitality levels as the molecule size ends up lesser and lesser is known as quantum restriction impact.

Quantum restriction effect

Built up mechanics, which treats electrons as particles, fail to explain the development of an electron around a center. Scientists by then recognized we need to consider an electron an atom, yet moreover as a wave. The wavelength (λ) of an electron is described as the de Broglie wavelength, and is given by the going with condition:

$$\lambda = \frac{h}{p} \text{ --------- (2)}$$

in which his the board's consistent and p is the energy of the electron. To be steady, the wave must recurrent its own example from past upset, or at the end of the day, the wave examples of each transformation must be in stage with one another . On the off chance that such a condition isn't met, every unrest will offset one another and in this way the wave won't stand. To fulfill this condition, it requires there to be a whole number of complete wavelength to make up one entire unrest. Along these lines, the wavelength of the electron must take

quantized qualities to fulfill the accompanying condition: nλ = a(1,2,3,…) in which an is the physical length of the space an electron is allowed to move.

The energy of the electron, which is corresponding to the proportional of wavelength square, likewise should take quantized qualities which is given by:

$$E = \frac{1}{\lambda^2} = \frac{n^2}{a^2} \text{----------(3)}$$

n =1,2,3,..

in which A will be a consistent. From the above conditions, we can see that the vitality dimensions of an electron must be An^2/a^2 and so forth., and they are isolated by energy contrast .In mass materials, for example, metals or graphite, electrons in the material are allowed to move anyplace inside the materials' physical measurement, and in such cases are huge. Subsequently, the vitality levels in mass materials are isolated by just a minor measure of vitality and they are basically persistent. In nanostructured materials, for example, GQDs, in any case, the electrons of the materials are bound to a little measurement an, and vitality levels isolated by

$$\frac{2(n-1)A}{a^2} \text{----------(4)}$$

become discrete and quantized, so quantum control impact ends up significant. Because of the quantum control impact, GQDs have enormous bandgaps and accordingly sharp absorbance tops and photoluminescence.

Chemical arrangement of GQDs

The substance arrangement of GQDs looks like that of graphene oxide. Like graphene oxide, GQDs are normally combined in an oxidative domain, so they are for the most part made out of the components of carbon, oxygen, and hydrogen. Because of the sulfuric corrosive and nitric corrosive ordinarily utilized in the blend, it isn't exceptional that GQDs contain a modest quantity of sulfur and nitrogen. During the decontamination venture of GQDs, monstrous heap of potassium hydroxide or sodium hydroxide are added to kill the acids. Preferably, the potassium or sodium salt shaped in the balance should be expelled during the dialysis step, however unavoidably there is a follow measure of metal particles left in the last items. The major heteroatoms other than hydrogen molecules in GQDs are oxygen particles. The noteworthy nearness of oxygen found in the GQDs originates from the different oxygen-

related useful gatherings including hydroxylic, carboxylic, epoxide, and carbonyl gatherings. In any case, the accurate amount of every oxygen-related useful gathering is hard to decide. In view of the covering pinnacles of these useful gatherings in FT-IR and XPS spectra, it's exceptionally testing to recognize one from others utilizing these two diagnostic procedures. NMR and mass spectrometry are likewise incredible assets in deciding substance structures of little natural particles, however the understanding of NMR and mass spectroscopic outcomes with graphene quantum dab isn't clear because of its basic multifaceted nature and high sub-atomic weight. What makes things increasingly troublesome is the way that synthetic organization of GQDs is subject to the amalgamation techniques, even a slight change in combination condition could prompt huge contrast in the items. Because of the assortment of engineered conditions scientists utilized in various labs, there has been a significant difference on the kinds of useful gatherings present on the carbon spine of GQDs. Starting at now, the nearness of epoxide or carboxyl gatherings is as yet not acknowledged by all.

Optical properties of GQDs

The optical property of GQDs is one of a kind, contrasted with different individuals in the carbon material family. In contrast to other carbon materials, GQDs have unmistakable retention tops and critical photoluminescence, because of their kept measurement as we examined before. The critical photoluminescence, alongside the low cyto-poisonous quality make GQDs reasonable for bio imaging [29-30]. However, GQDs regularly radiate green or blue hued photons, while longer wavelength discharges, for example, red or close IR photons are progressively attractive for bio imaging applications since they have a more drawn out infiltration profundity through organic tissues. The outflow wavelength of GQDs is subject to the size and useful gatherings.

For the most part, with an expanding conjugation length of the chromophore, or with expanding level of functionalization, GQDs show progressively red-moved outflow. By the by, the photoluminescence component of GQDs isn't completely comprehended and the exact tuning of their photoluminescence has not been accomplished.

Size impact:

Size impact is basically quantum control impact. From our previous discourse on quantum control impact, we realize that a littler size of a GQD atom prompts a bigger bandgap, which result in shorter wavelength photoluminescence. This contention bodes well and is upheld by trial confirmations. Fuyuno [31] and collaborators isolated as-arranged GQDs into various size-appropriated bunches by means of fluid chromatography.

As indicated by their outcomes, enormous estimated GQDs radiate at longer wavelength than littler measured GQDs. In spite of the fact that the size impact on the outflow of GQDs has been commonly acknowledged in the exploration network, some examination gathering discovered confirmations showing that size isn't the main factor adding to the emanation properties. Tang [32] and colleagues discovered size independent discharge of 3.2 nm, 10.7 nm, 21.0 nm GQDs.They credited the commanding variable in the outflow of GQDs to be emissive snares incited by surface conditions of the utilitarian gatherings. Yeh [33] and collaborators utilized hypothetical computation to assess the bandgaps of GQDs of different sizes, and contrasted that and test estimations.

As can be found in Fig 4, GQDs in the estimation show a lot bigger bandgaps than the anticipated qualities by computation, demonstrating GQDs to have an a lot littler sp^2 conjugation space than their external measurement [33]. Specifically, trial results from our investigation with single molecule photoluminescence method gave a solid proof that multi-chromophoric discharge may happen from GQDs [34]. In a rundown, albeit size impact on the outflow of GQDs remains commonly substantial, one can't definitely tune the emanation of GQDs by exclusively controlling their sizes, because of the unpredictable nature in the outflow of GQDs.

Effect of Defects

Another mainstream approach in clarifying the photoluminescence properties of GQDs is through their imperfection destinations. As we talked about before, the normal readiness techniques for GQDs award them a noteworthy amount of surface practical gatherings. These useful gatherings fill in as imperfection locales and can significantly change the photoluminescence properties of GQDs. Contrasted with the size impact, there has been considerably more discussions and differences in how useful gatherings influence optical properties of GQDs. The purpose behind the irregularity among research gatherings lies in

the way that it is for all intents and purposes extremely testing to unequivocally portray the sorts and amount of utilitarian gatherings on GQDs. Since research gatherings utilize various techniques to set up their own GQDs, they ordinarily end up contemplating GQDs of various structures. Li [35] and colleagues electrochemically doped nitrogen to oxygen-rich GQDs, and discovered 50 nm blue move in discharge contrasted with sans nitrogen counterpart. Tetsuka [36] and collaborators functionalize GQDs with essential amines, and tuned the outflow of GQDs from violet to yellow through the degree of functionalization.A blue-moved emanation and the expansion of a quantum yield are frequently seen with substance decrease of GQDs. Surface passivation by appending long chain polymers anxious oxygen useful gathering is additionally connected with the noteworthy improvement of emanation quantum yield.

CHAPTER 2 LITERATURE REVIEW

The principal single layer graphene was extricated from profoundly situated pyrolytic graphite by Andre Geim and Kostya Novoselov [4] utilizing the scotch tape. As of not long ago, there is no procedure built up that can make graphene test with such high bearer versatility and low thickness of deformities [9]. Be that as it may, mechanical shedding is restricted underway scale and tedious. This hindrance restrains the application to principal research of graphene. After over 10 years' advancement, for the present mechanical generation of graphene, there are two noteworthy blend courses: base up epitaxial development and top-down peeling [10]. The base up epitaxial development approach includes the immediate union of graphene materials from the carbon sources [10]. A normal technique, for instance, is the compound vapor deposition (CVD). CVD is generally used to develop enormous scale, single or multi-layer graphene sheets on metal substrates with low imperfections thickness [10, 11]. In an unexpected way, the top-down methodologies, for example, decrease of graphene oxide (GO) take preferences of high return, simplicity of usage, and arrangement based procedure capacity [10,12]. Specifically, the minimal effort and large scale manufacturing of decreased graphene oxide sheets has been acknowledged [10,13]. Among these strategies, decrease of graphene oxide (GO) was believed to be a standout amongst the most noticeable techniques to accomplish the huge scale and minimal effort generation of graphene [13]. GO as an exceptionally oxidized sheet is incorporated from solid oxidation of immaculate graphite pursued by mechanical peeling, for example, ultra-sonication in fluid media or simply mixing [13,14]. The π system of the graphene adds to the conductivity for graphene, so the GO must be reduced or converted to other dimensions to regain its π bond [26]. The GO are typically decreased by electrochemical,thermal or chemical processes [26]. The byproducts don't have very high quality as a result of the nearness of extraneous imperfections (oxygen gatherings) and natural imperfections (edges), however this technique permits the creation with high return and generally low expenses. In this manner, oxidation of graphite, mechanical shedding and decrease of GO are the well-known techniques to create industrial graphene. The most prominent techniques detailed as of late are chemical vapor deposition (CVD) or plasma improved synthetic route of chemical vapor deposition (PECVD) which can deliver huge scale and moderate quality graphene films.

S. Bae et al [37] have built up a procedure to fabricate 30 inch graphene film on copper by utilizing rolling technique in 2010. From that point forward, SONY [38] has orchestrated 100 meter long graphene film utilizing the comparative strategy in 2013. Be that as it may, the graphene inclusion isn't uniform and diminishes when close to the film edge. Additionally, there are imperfections brought about by plastically twisting of copper foil. These non-unimportant imperfections break the intermittent structure and lower the conductivity of graphene [38]. Despite the fact that in 2015 another technique called Concentric Tube CVD created by Polsen, E.S. et al. [39] has improved the generation speed and quality, the expense of CVD techniques are still too high thinking about the low yield.

Graphene oxide (GO) has a comparative structure to graphene. Both of these mixes have a hexagonal carbon cross section, yet the GO sheet is normally mutilated where it is attached to the oxygen gatherings. GO as one of the source materials for enormous scale creation of graphene has been contemplated for a considerable length of time. There are numerous applications for GO, for example, potential materials for anode in Li-particle batteries [9], straightforward conductor in natural photovoltaic cells [40]. Regardless of these propelled application, the key assurance of the structure of GO has been moderate. Scientists have proposed numerous hypothetical models for GO however the exact substance structure is as yet questionable. Real reasons incorporate example to-test fluctuation because of various strategies involved in the degree of oxidation, the measure of amorphization, the nonstoichiometric idea of GO, and the restricted goals in the real portrayal procedures, for example, SSNMR and FTIR. In any case, the assurance of the exact structure of GO is as yet deserving of study since it will surely improve the comprehension of the functionalization and decrease procedure of GO. In 2008, Ruoff's team [41] arranged a C^{13} - advanced GO test and three wide resonances at 60, 70 and 130 ppm were found in the C^{13} SSNMR range.From that point onward, SSNMR demonstrated to be a standout amongst the most exact and dependable methods to describe GO structure. As indicated by the portrayal above, past analysts have proposed in any event 5 exemplary structure models (Fig 6) [36-45].In 2005, Décány's [42] research group built up the DRIFT investigation and explained real pinnacles of a GO test made by Brodie strategy [43]. They recognized the hydroxyl signals from water and in this manner end the past discussion on GO FTIR results. UV-vis range indicates two appointed groups at 234 nm and 299 nm, coming about because of the π to π^* change of fragrant carbon bonds C=C and n to $\pi*$ progress of C=O bonds [44]. In the X-ray beam diffraction spectroscopy,GO generally demonstrates an extensive top at 10.2 degrees

perceived from graphene at 16.7 degrees [45].Transmission Electron Microscopy (TEM) and Atomic Force Microscopy (AFM) uncovers the two dimensional structure of GO. TEM could without much of a stretch affirm the hexagonal graphene-like cross section of GO while the AFM watched a harshness of in any event 0.6 nm on GO surface.

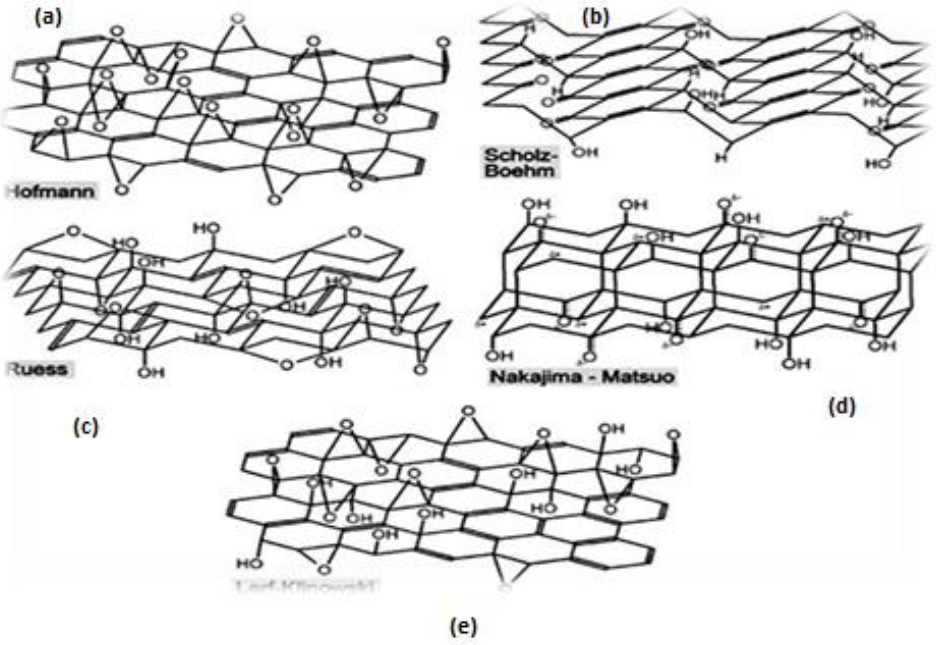

Figure 6: The five different structures of GO which are studied and reported are (a) Hoffman.(b) Scholz-Boehm.(c) Ruess.(d) Nakajima-Matsuo.(e) Lerf-Klinowski [46].

The principal model as given by Hofmann and Holst [42] in 1939 portrays a level carbon sheet haphazardly reinforced with epoxy bunches with a C/O proportion of 2. At that point in 1946, Ruess' [49] gathering presented the hydroxyl gatherings and 1, 3-ether to the grid .The grid is formed by cyclohexane rings which are not quite the same as Hofmann's benzene-like carbon plane. Scholz-Boehm's model [48] totally replaces the epoxide bunches with hydroxyl gatherings. The basal plane is ordinary folded cyclohexane rings connected with a quinoidal structure.Nakajima and Matsuo [50] 1994, manufactured a grid structure similar to poly $(C_2F)_n$ which structures a two phase graphite intercalation compound. Nonetheless, the most recent two models proposed by Lerf-Klinowski [40] and Décány [42] have turned out to be most well known in light of the fact that the SSNMR examination was brought into GO structure portrayal. This new method has improved the precision in distinguishing the practical gatherings on GO. In the Lerf-Klinowski (LK) model [46], tertiary alcohols and 1, 2-ethers are predominant gatherings in a hurry surface. The LK model disposes of the occasional gem structure and substituted by the arbitrarily appropriated oxygen gatherings.

They additionally recommended that the alkenes (C=C) in GO are most likely either pleasant odour or conjugated and ketones are increasingly ideal at the edge of GO. Afterward, Décány [42]proposed a model after the essential rationale of Scholz-Bohm [47] model, yet including 1,3-ethers into the cyclohexane rings.

Despite such numerous hypothetical models, the genuine structure of GO still stays dubious. One reason might be that these models arranges the oxygen bunches physically in a fixed cell inside a restricted scale. Be that as it may, the genuine GO structure is non-stoichiometric and non-intermittent in the long range.

On the off chance that GQD combination is considered in its early stages, one might say that the functionalisation and gathering of GQDs are at their origination. Functionalisation of GQDs can possibly adjust photoluminescence, biocompatibility and conductivity so that the quantum yield and other parameters like optical, electronic etc are upgraded. Functionalisation has likewise been appeared to create GQDs with conspicuous up-change and with great quantum yields. Like the strategies used to deliver GQDs, change of GQDs can be accomplished by two unique methodologies; pre-creation alteration of parent materials and adjustment post GQD blend, named post-manufacture adjustment . In this area, we portray these techniques in more detail. Lu et al [52] framed little nanodots through the Rh-catalyzed confine hole of fullerene. The Rh surface cooperates firmly with the buckminsterfullerene atoms, prompting tiny openings over Rh, that encourages the fullerene particles to get accumulated on the surface. The discontinuity of the inserted particles at raised temperatures at that point produces carbon bunches that experience dissemination and conglomeration to frame graphene nanodots. By advancing the toughening temperature the state of the GQDs can be tailored. Sun et al.[45] offered another approach to improve photoluminescence characteristics of graphene nanodots as opposed to the much announced concoction decrease and surface passivation. They created GQDs having fluoroscence towards blue region by photograph decrease utilizing isopropanol. This gave a 3.76 crease increment in the QY among photograph decreased and artificially diminished GQDs.In expansion to the expansion in QY, this strategy likewise has the benefit of a lot shorter response times for this decrease step (a few minutes rather than a few hours) and keeps away from poisonous reagents.

Feng' et al.[53] sliced the fluorine containing graphene hydrothermally to deliver fluorine comprising GQDs with a nuclear proportion of ca. 23.7 %, with functional-rich utilitarian

gatherings. Like N'- doped graphene nanodots, fluorinated graphene nanodots also alters various characteristics like the optoelectronic properties of graphene nanodots, and showed clean up-transformation with iridescence properties and electronic advances like those saw in N'-doped GQDs. Liu et al.[45] created glutathione-functionalised GQDs (GQDs-Gsh') by means of a one-advance pyrolysis technique. Citrus extract and glutatione (Gsh' – a tripeptide containing glycne, cystine and glutamate) were blended, warmed, broke up into millipure-Q ultrapure water and isolated by means of section chromatography, creating GQDs-Gsh' along sizes going from 6 – 60 nm. The glutatione functionalisation was likewise appeared to improve both natural similarity and fluorescence QY (~ 33.60 %).

CHAPTER 3 : EXPERIMENTAL SECTION

3.1) Materials and Methods undertaken.

The materials utilized throughout the work were of scientific evaluation and standard and were used without performing any further purification. Graphite powder was purchased from CDH. Potassium permanganate ($KMnO_4$) was bought from RANKEM, The acids used are sulphuric acid(H_2SO_4 concentration 98%), hydrochloric acid (HCl concentration 35.86 %), hydrogen peroxide (H_2O_2) and nitric acid (HNO_3). Ethanol (CH_3CH_2OH) was purchased from changshu yangyuan chemical and distilled water (DI) was used throughout the process.

Perkin Elmer LAMBDA-750 UV-Visible-IR spectrophotometer is the instrument utilized for recording UV-Vis absorption spectra. Horiba jobin Yvon inc. Fluorolog-3 spectrofluorometer records the photoluminescence of the sample. FEI Technai F20 ST Transmission electron microscope takes the TEM pictures performed at 200 kV. FT-IR images were taken with the help of Perkin Elmer spectrum 65 FT-IR spectrometer.

3.2)Graphene Oxide

3.2.1) Reaction Set-up

(a)

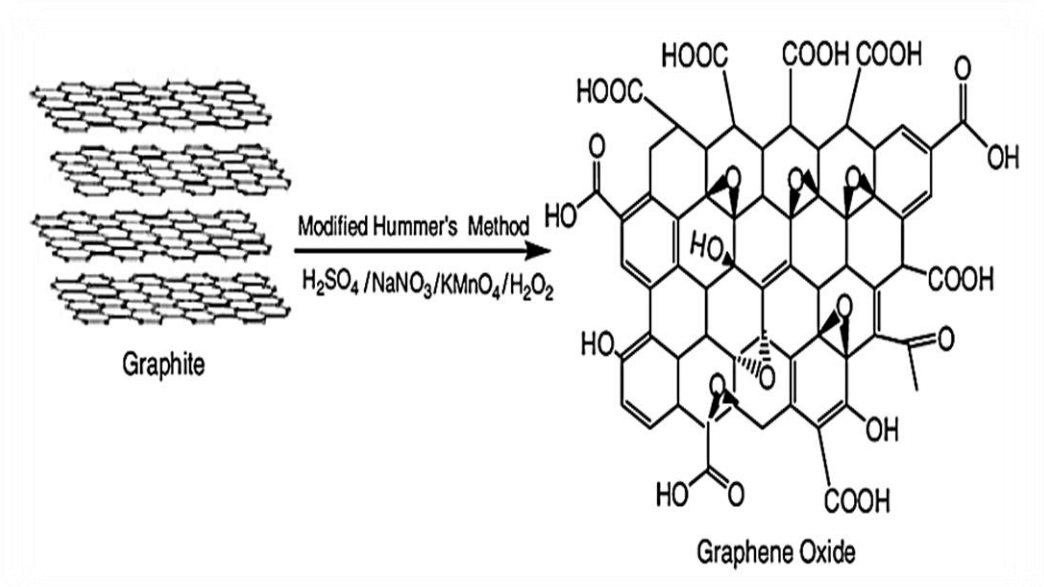

(b)

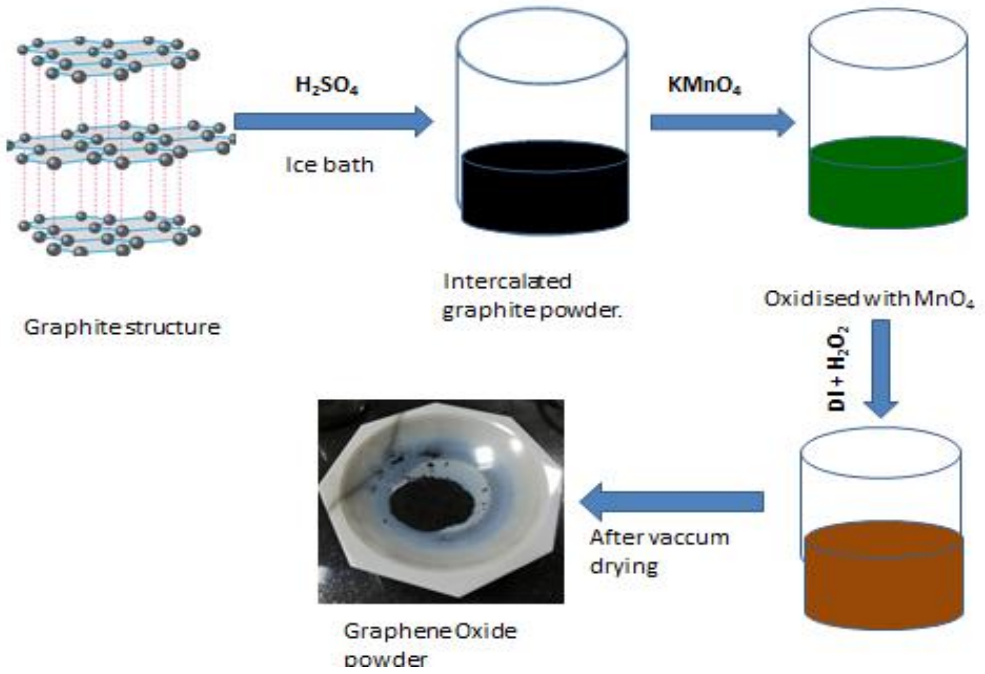

Fig 7-(a)Structural changes from graphite to graphene oxide when synthesized through modified hummers method.(b)Process flow diagram for synthesizing GO.

The entire process is divided in three temperature stages [fig 8].

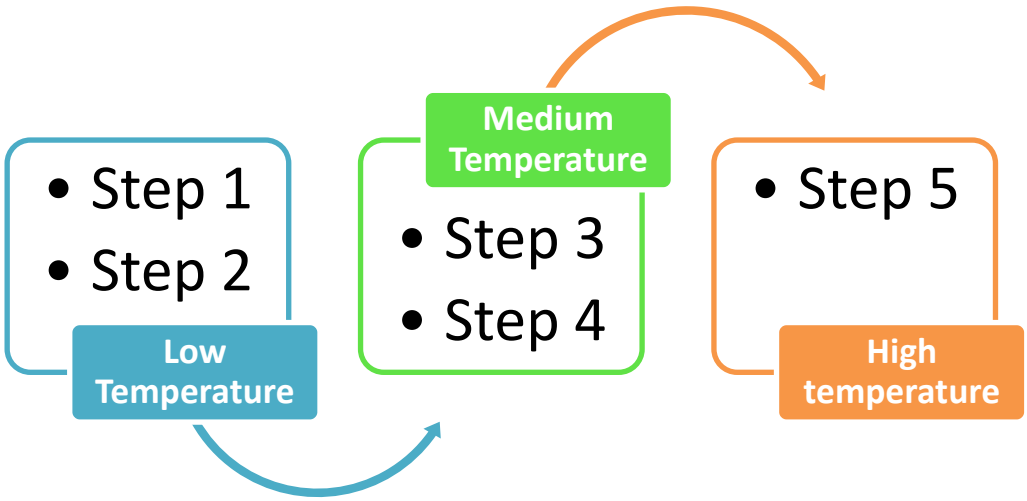

Fig 8: The different temperature zones present in modified hummers method.

3.2.2) Method Used.

Modified Hummers method [52] was undertaken in the synthesis and production of Graphene Oxide (GO). The changes in structure are shown in fig 7 (a) and (b) .The steps followed for their synthesis are illustrated below :

Procedure :

1. 1 gram of graphite powder was added in a beaker containing 50 ml of sulphuric acid kept in an ice-bath and stirred for 30 minutes.
2. 6 grams of potassium permanganate was added slowly to the container with continuous stirring.
3. After complete addition of $KMnO_4$ ice bath was removed and the temperature was increased to 30˚ C and stirred for 1 hour.
4. After a duration of 1 hour, 80 ml Millipore distilled water was slowly added with rigorous stirring and a lot of effervescence was observed.
5. The temperature of the container was now increased to 90˚ C and stirred for 30 minutes.
6. To stop the reaction 200 ml of Millipore distilled water and 20 ml of hydrogen peroxide was added and the solution was kept separated to cool down for 24 hours.
   As the reaction stops, a highly impure GO dissolved in water is obtained.

PART TWO

The washing and filtering steps to obtain a highly pure GO required a larger duration as it was a very stable colloid.

7. After leaving the solution for 48 hours, a black accumulation is observed on the lower part of the container and a clear solution on the upper part. The supernatant was removed from the beaker to another vessel.
8. After adding 10 ml HCl to remove the Mn^{2+} and Cl^- ions from the solution, centrifugation was performed at 6000 rpm and the residue was collected.
9. The above step is repeated three to five times with distilled water and ethanol so that all the unwanted ions are washed away.
10. Highly acidic solution of GO is obtained which is neutralized by adding 0.1 M NaOH solution.

11. Powdered GO was obtained by removing the excessive water at 40˚ C in a confined vacuum space.

3.2) Graphene Quantum Dots (GQDs).

3.2.1) Reaction Set up

(a)

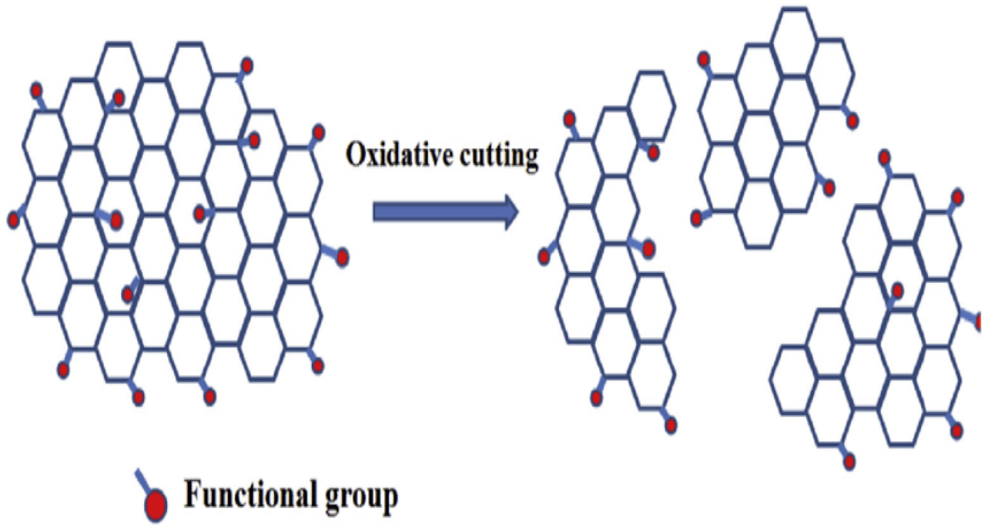

(b)

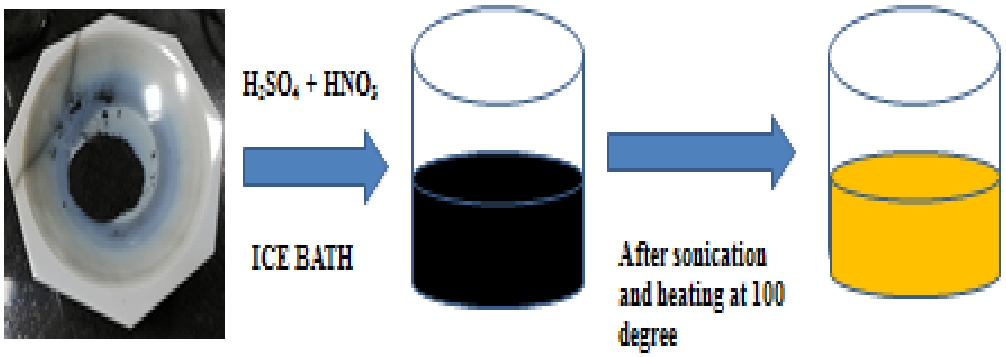

Fig 9:(a)Oxidative cutting of graphene oxide by strong acids to synthesize graphene quantum dots [51].(b)Process flow diagram for synthesizing GQDs.

3.2.2) Method Used

Oxidative cutting method was utilized to synthesize graphene quantum dots [fig 9 (a) and (b)]. The steps followed are illustrated below:

1. 0.2 grams of GO was added in 30 ml of H_2SO_4 and 10 ml of HNO_3 and stirred continuously for 60 minutes.
2. The mixture was sonicated for 120 minutes by completely covering the beaker.
3. The temperature was raised to 100˚ C and stirred continuously for 3 hours.
4. It was kept aside for 24 hours so that all the heat gets removed and the solution comes to room temperature.
5. 40 ml distilled water and 0.1M NaOH solution was added to make the pH neutral.
6. The solution was filtered and centrifuged to remove all the GO residue left behind.
7. A pale yellow solution containing GQDs was obtained as the end product.

CHAPTER 4 : CHARACTERIZATION TECHNIQUES

1. UV-Visible-IR spectrophotometer :

Fig 10: UV-Vis-IR Spectrophotometer
(Model: Perkin Elmer 750 LAMBDA)

Depending on the different qualities of synthetic mixes present in the nature they carry on diversely when electromagnetic waves fall on them. They either reflect, assimilate or transmits a specific area of recurrence or wavelength. Spectrophotometer [fig 10 and 11] is an investigation system which causes us in deciding how much a material transmits or assimilates a specific area of electromagnetic wave. By and large there are two exceptionally well known kind of spectrophotometer. One is atomic discharge spectrophotometry and the other nuclear absorption spectrophotometry. This system or gear fundamentally figures the amount of photons ingested when the example arrangement is exposed to the way of these photons. Each compound substance has a specific wavelength which it retains and hence this strategy causes us in discovering that absorbance pinnacle of the substance. Contingent on the scope of wavelength that is utilized, it very well may be portrayed in two sorts:

- **UV-Visible spectrophotometer :** This operates in the ultraviolet range (190nm-400nm) and visible range (400nm-700nm) of EM radiation spectrum.
- **IR spectrophotometer :** The operating range is the infrared region (700nm-3200 nm) of EM radiation spectrum.

Principle : The Beer-Lamb'ert hypothesis expresses that the absorption of a material in the form of solution is straightforwardly corresponding to the grouping of the retaining species in the mixture and in the distance they traverse .Accordingly, for a standard mean way length, UV-Vis spectrometer can be utilized to decide the amount of the absorbing material in the prepared sample. The absorption changes with amount of the sample present in the solution. This can be taken from standards (tables of molar annihilation coefficients), or all the more precisely, decided by an adjustment bend.

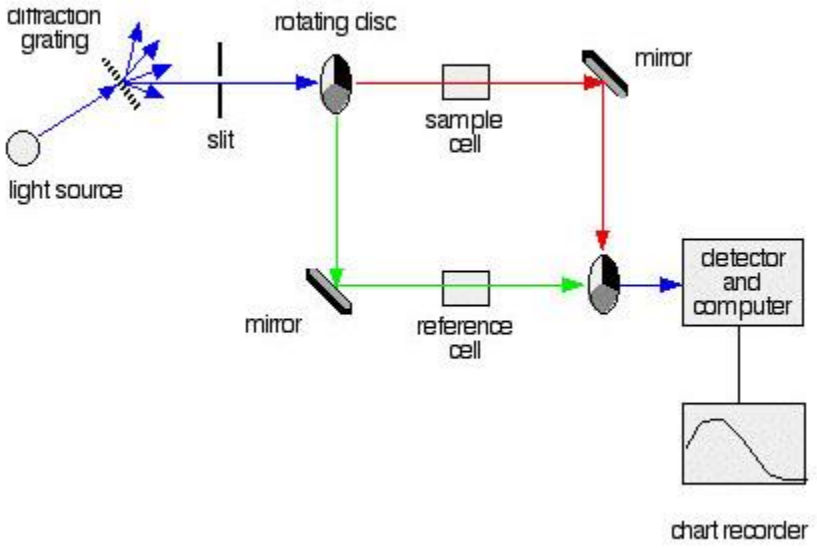

Fig 11: Schematic representation of double beam spectrophotometer.

i)The lamp source

A lamp source is required which creates the whole range of visible spectrum in addition to the close ultra-violet and infra-red region with the goal that we are traversing the range from around 190 nm to around 3200 nm.You cannot accumulate this scope of frequencies from a solitary light, thus a mix of both is utilized - a deuterium' light for the ultraviolet component of the range, and a incandescent light for the white range. The consolidated yield of both these lamps is striked on to a diffraction grinding.

ii) Slit and the diffraction grating

You are most likely acquainted with the manner in which that a crystal parts light into its segment hues. A diffraction grinding does likewise work, yet more proficiently. The blue

bolts demonstrate the manner in which the different ranges of the lamp are given off in various ways. The cut just permits range of a limited scope of wavelength values onto the remainder of the spectro-photometer. By step by step turning the diffraction grinding, you can permit light from the entire range (a small piece of the range at any given moment) through into the remainder of the instrument. By bit by bit pivoting the diffraction grinding, you can permit light from the entire range (a little section of wavelength at any given moment) through into the remainder of the set-up.

iii) The circulating plates

This is the most important piece! Each plate is comprised of various portions. The ones present in the set-up we are portraying have three distinct areas - varied manufacturers might have an alternate serial. The photons originating from the diffraction grinding and cut strike the turning plate and three of the various things can take place. If they strike the straightforward segment, it will travel right through and go along the compartment containing the solution. It is then bobbed with a plane glass on a secondary turning disc. This plate is pivoting with the end goal that when the photons touches base from the principal circle, it interacts with the reflected segment of the subsequent plate. Then they bobs it onto the output collector. If the first light emission of the cut targets the reflected segment of the primary pivoting circle, it is bobbed downwards in the green range. After the plane glass, it goes through a standard compartment. At last the photons travels to the secondary plate which is turning so that it interacts the straightforward segment. It travels lineraly through to the locator. Ultimately the photons strikes the main circle in the dark area, it is stopped and for a brief time no photon is allowed through the spectro-photometer. Therefore, the fair enables the PC to offer wait time for any voltage produced by the identifier without any light.

iv)The reference and sample compartments

These are little cubical quartz compartments. They are frequently structured so the photons traverses a separation of 1 cm along the given direction of the sample. The testing compartments contain an answer of the sample solution we are trying - generally exceptionally weaken. The material on which the sample is dissolved is picked so it doesnot

retain any critical measure of photons in the range of wavelength extend(200-800 nm).The standard compartment involves the unadulterated spectrum of pure solvent i.e. used.

v) The demodulator and the PC

The indicator changes over the approaching photons into a electrical signal. More the value of the electrical impulse, the more prominent the strength of the photons. For every region of light wavelengths traversing along the spectro-photometer, the force of the photons traversing through the standard compartment is estimated. This is generally alluded to as $I_{\circ}$i.e. I for Intensity.The power of the photons travelling towards the example compartments is additionally estimated for that range or region – taken from the image, I. If I is not very close to value of $I_{\circ}$, at that instant clearly the sample has assimilated a region of the photons. A rightful analysis and calculations is then performed in the desktop to revise the value so that it can be standardized for everybody using the standard as absorbance - given the graph, A. For reasons which will progress toward becoming more clear if we complete a touch of hypothesis on another value, the connection among An and the two powers is given by:

$$A = \log_e\left(\frac{I_{\circ}}{I}\right) \text{ ----------(5)}$$

Over the vast majority of the outlines we will encompass over, the value of absorbance traverses over 0 to 1, however it can even attains higher value than that. A value of zero at some wavelength implies that no photons of that given frequency has been retained. The powers of the example and standard shaft both are equivalent, therefore the proportion $I_{\circ}/I$ is one. Log_{10} of one is zero. An absorption value of one appears when 90 percentage of the photons at that range has been assimilated - which implies that the power is 10 percentage of the photons traversed some way or another be.In that case, $I_{\circ}/I$ is 100/Io (=10).

2) Spectrofluorometer :

A spectrofluorometer is an instrument which takes resources of fluorescent properties of few mixes so as to contribute data concerning their focus and synthetic environment in an example. Some excitation wavelength is picked, and the discharge is perceived either at an interesting wavelength, or a sweep is executed to take note of the power versus wavelength, for example outflow spectra.

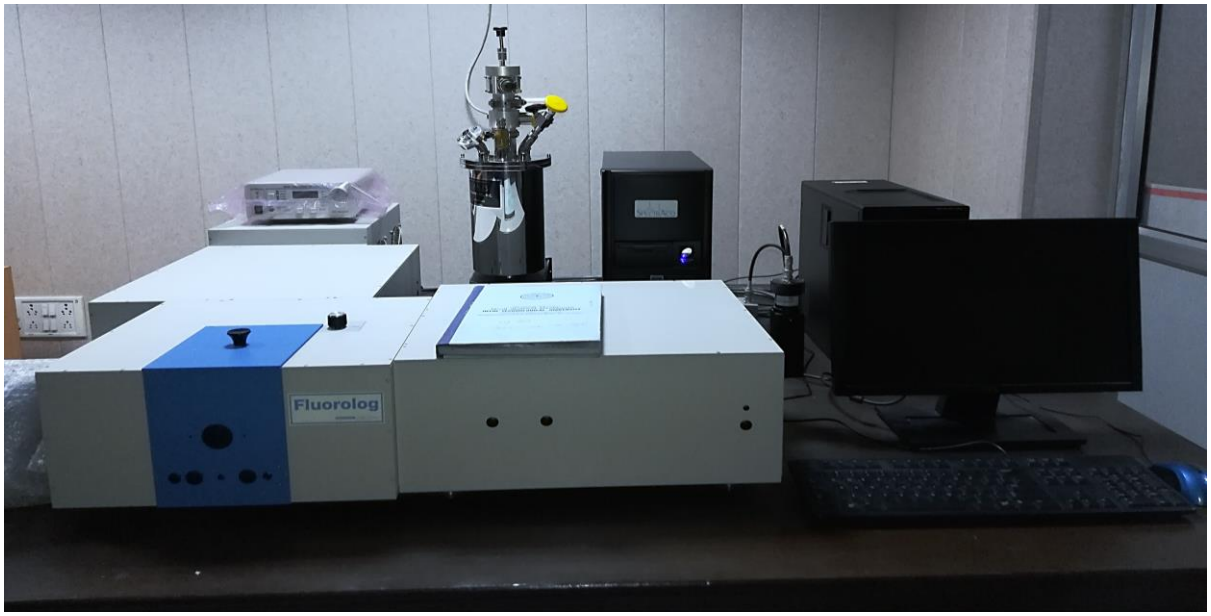

Fig 12: Fluorolog-3,Horiba Jobin Yvon Inc spectroflurometer

With most spectrofluorometers, it is practical to watch both excitation as well as emission spectra. An excitation range thoroughly relies upon the outflow force, since it is estimated at a solitary emanation wavelength. Alternately, a discharge range absolutely relies upon the excitation wavelength. Such produced spectra can be spoken to on either a wavenumber scale or a wavelength scale. Normally, emanation/PL of a given vitality can be appeared as far as its wavelength(λ), wavenumber or recurrence (v). The general units for wavelength are in nanometers and wavenumbers are in cm^{-1}. For an ideal instrument, the unequivocally recorded discharge spectra would show power radiated at every wavelength or the photon outflow rate, over an interim of wavelength settled by the cut expansiveness and scattering of the emanation monochromator [fig 13].Similarly, at every excitation wavelength the excitation range demonstrates the general discharge of the fluorophore .For most fluorophores, the discharge/PL spectra and quantum yields are isolated from excitation wavelength. Accordingly, the excitation range of an example arrangement can be cover on its retention range. In any case, such similar retention and excitation spectra are infrequently watched in light of the fact that the excitation power is unmistakable at every wavelength. Indeed, even under ideal conditions such closeness of the excitation and retention spectra requires the presence of just an exceptional sort of fluorophore, and the nonappearance of other confusable variables.

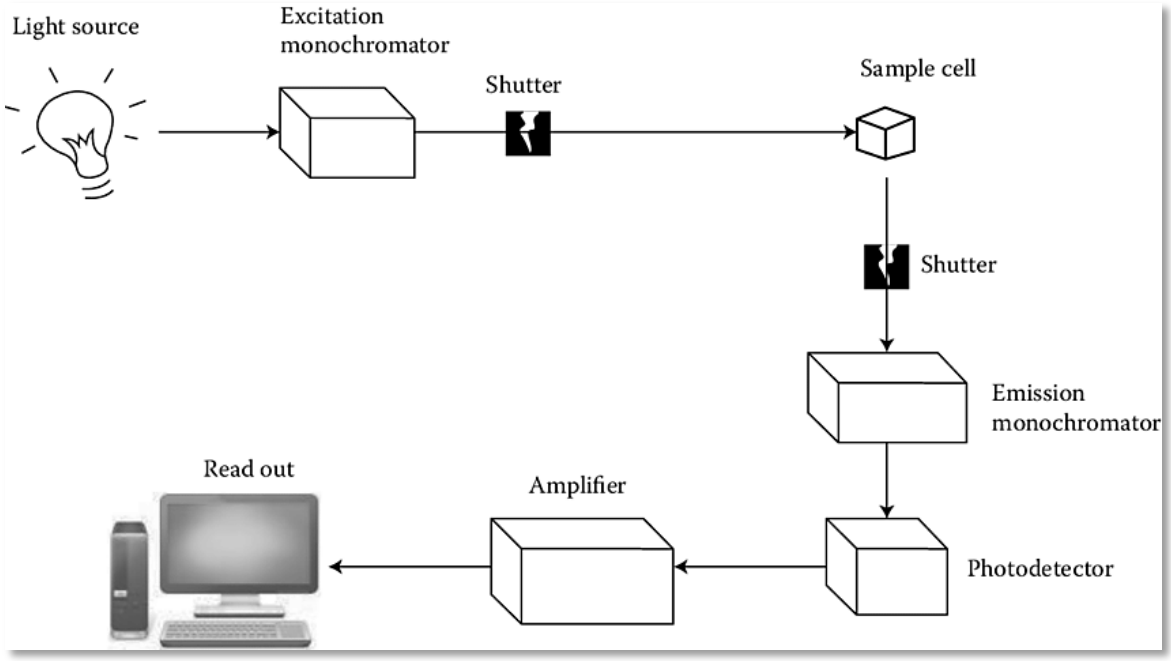

Fig 13: Schematic representation of spectrofluorometer

Outflow spectra recorded on particular instruments can be unmistakable on the grounds that instruments are wavelength touchy. The Horiba Yvon Inc. Fluorolog-3[Fig 12] is a spectrofluorometer comprising xenon circular segment lights as a light wellspring of 450 w generally helpful on account of their tremendous power at all wavelengths running from 200 nm, double monochromators to world class both the excitation and discharge wavelengths. Moreover, curved gratings are utilized by these monochromators, produced by holographic intends to decreasing stray light. An example area with a cuvette holder and a photomultiplier tube(PMT) for the discovery of fluorescence and after that deliberate it with appropriate electronic gadgets. The yield is commonly spoken to in the graphical structure.

3) X-ray Diffraction Method(XRD).

X-ray powder diffractometer (XRD) [fig 14] is a speedy logical technique fundamentally used for level conspicuous verification of a crystalline substance and can give information on single cell approximations. The analyzed matter is accurately grounded, homogenized, and average composed and setup of mass material is resolved.

Fig 14: X-ray Diffractometer
[Model : Bruker's D8 Discover]

Basic Concept :. Max von Laue, in 1912, found that substances having crystallity popularly travel through as 3-D diffraction grindings for X-shaft ranges like the dislocations of planes in a cross-sectional circle. Currently X-shaft diffraction is regarded as a typical way for the cross examination of precious stone structures and nuclear spacings [fig 15]. Depending on productive interruption of paths of monochromatic beams and the standard substances these beams are created by a CRT, which are kept to deliver monochromatic energies, generally they are collimated so that they can strike, and synchronized with the example. The relationship between the originating beams with the example produces impedance (and a diffracted shaft) fulfilling the Bragg's Law conditions

$$n\lambda=2d \sin \theta \text{----------(6)}$$

This hypothesis tries to connect the wavelength of em radiation to the diffraction values observed and the cross sectional divisions of a crystalline standard. After identification these beams are allowed to traverse and then tallied. Upon studying the 2 theta angles and comparing them with the standard ZnO samples we get to know about the various diffraction values that are obtained. This technique helps us in evaluating layer separations present inside the material d. We can even determine the various domains present inside the sample, their homogeneity. The average width regarding their crystallinity can also be calculated from the peak values obtained in the XRD pattern. The in-plane periodic crystallinity of the plane can

also be observed and even the number of layers of the sample present can be evaluated. While observing all these we generally use $CuK\alpha^1$ and $CuK\alpha^2$ as standards for wavelengths which helps in calculating various mathematical formulas and even help in determining FWHM of the sample.

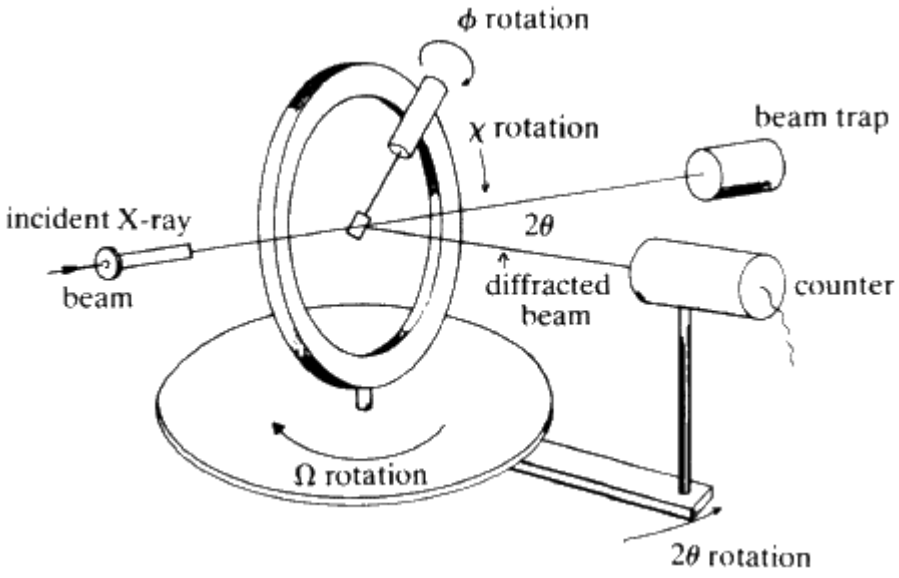

Fig 15: Schematic diagram of XRD working.

4) Fourier Transform Infrared Spectroscopy

This technique is basically used to get an infra-red range retention of a chemical compound present in any of the three forms. A FT-IR spectrophotometer [fig 16] at the same time accumulates high-spectral resolution values ranging over a wide wavenumber. This provides benefit of a large scale over a dispersive spectrophotometer, which traverses over a limited region of wavelength for calculating power with the duration of time. It basically ranges over a region and tries to collect information about the various bonds present in the sample. Generally it is used to determine various functional groups that are present in the compounds. This is a very important technique which provides us vital informations about the internal bonds present in our sample.

Fig 16: FT-IR spectrometer
[Model : Tensor 27]

Basic Principle :

The basic working of FT-IR is based upon atomic and molecular vibrations. The various atoms present in a compound have different vibrational energies which completely depends upon their bonds and their structures. These frequencies are basically related to either their ground states or a few energized state which is given by Quantum mechnics. One way we have re-introduce vibrations in these atoms is by energizing them to the higher states so that it's energy is retained. Randomly, they should always rise from their ground state to the higher levels for having vibrations which can give us clear distinctions between their bonds. Thus, in FT-IR we generally provide them the required energy in the form of light source so that they can get energized and vibrate so that we can get their values.They generally have quite unique characteistics like high affectability execution with the for all time adjusted, high shape corner interferometer, adaptable workspaces, hyperspectral photos,the rmogravimetric coupling, high throughput screening gadgets and simple estimation mode.

5) Transmission Electron Microscopy (TEM) :

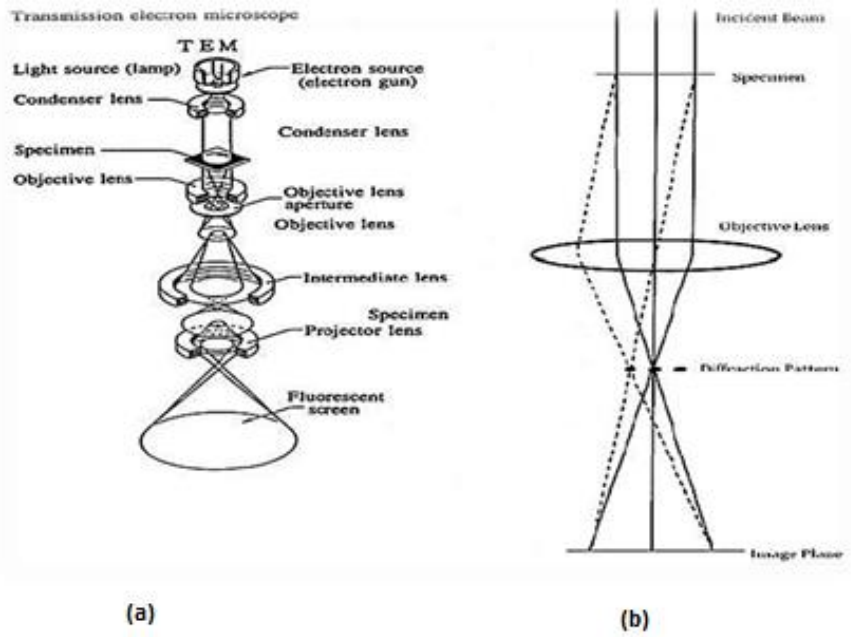

Fig 17:(a)Schematic diagram of TEM. (b) A ray diagram for the diffraction mechanism in TEM.

Principle :

The TEM [fig 17 (a) and (b)] is a method which helps material scientists in determining the surface characteristics of their sample. Generally electrons are passed from the guns to the sample which are adjusted by different condenser lenses which help the beam to fall on the required sample and thus help in maintain the direction and travelling path of the ray. We use electrons over photon sources as they can penetrate over deeper wavelengths compared to them. In contrast to SEM, the Tem images are more precise in terms of internal parameters and imaging. A fluorescent screen is kept just below the specimen sample so that a high fidelity image can be obtained. Generally a voltage of 220kV is provided from the gun. It helps us in determining the deformities and impurities that are also produced along with the sample. These are high accuracy and resolution images which confirms the production of the required product. They are generally for determining nanosamples like particles and quantum dots. All type of nano scale images like quantum dots, wells, wires, rods etc can be easily observed in TEM with great precision.

A) The photo generation stage

When light is emitted in the form of electrons from the electron gun they traverse a path guided by various condenser lenses so that they don't deviate from their path and travel directly to the specimen kept at the end whose image is to be determined. There are condenser holes which restricts high point electrons. The beam then strikes the sample and traverse through it depending completely on the thickness of the specimen. There is a phosphor screen or CCD camera where the transmitted beam strikes and creates a diffracted image of the specimen traversed. There are additional focal points which helps in improving the image quality of the picture. As the picture strikes the screen, certain amount of light is produced which helps the user to see the image of the surface of the specimen. The dark regions of the image represents that lesser electrons were transmitted through this region while the lighter region stands for more transmitted electrons. The major difference between SEM and TEM is that in the former back scattered electrons were used to create the image while in TEM transmitted electrons create the image.

B) Specimen Preparation

A TEM example must be thin enough to transmit adequate electrons to shape a picture with least energy loss. Consequently example readiness is a significant part of the TEM investigation. For most electronic materials, a typical arrangement of readiness systems is ultrasonic plate cutting, dimpling, and particle processing. Dimpling is a planning system that delivers an example with a diminished focal zone and an external edge of adequate thickness to allow simplicity of taking care of. Particle processing is customarily the last type of example readiness. In this procedure, charged argon particles are quickened to the example surface by the utilization of high voltage. The particle impingement upon the example surface evacuates material because of force move

Chapter 5 : RESULTS & DISCUSSIONS

5.1) Graphene Oxide (GO)

After following all the steps of modified hummers method, powdered GO is obtained which is black in colour and have neutral pH [fig 18] .

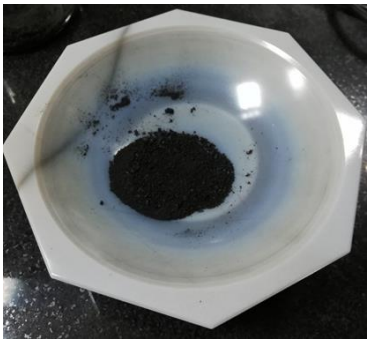

Fig 18 : The GO powder produced by modified hummers method.

The samples for the various characterizations were prepared by mixing 0.02g of GO in 5 ml of distilled water. It was then ultra sonicated for 90 minutes to maintain the uniformity of the solution. It was diluted with 0.1 M NaOH or HCl to make the solution either alkaline or acidic depending on the requirement. The UV-Vis absorption spectra of GO suspended in distilled water in 2 mm cuvette ranging over a wavelength of 200-700 nm at pH 8, 1 and 14 are measured [fig 19 (a,b,c)].

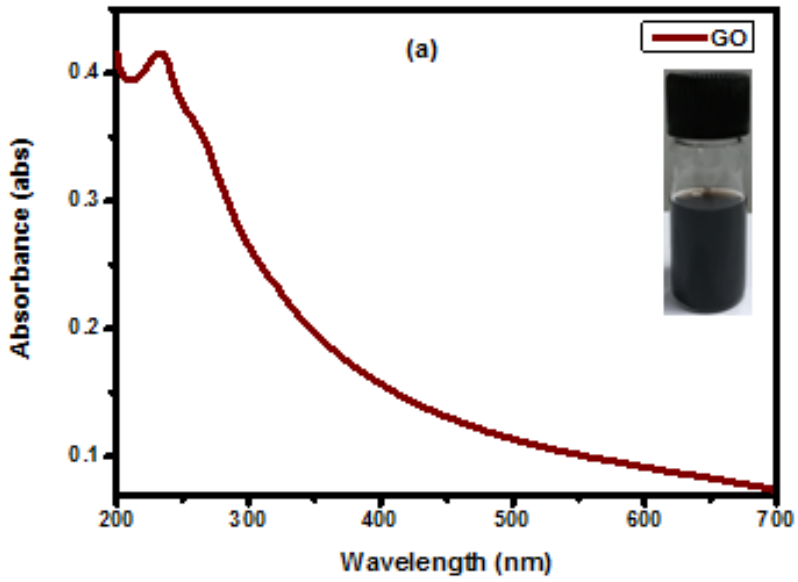

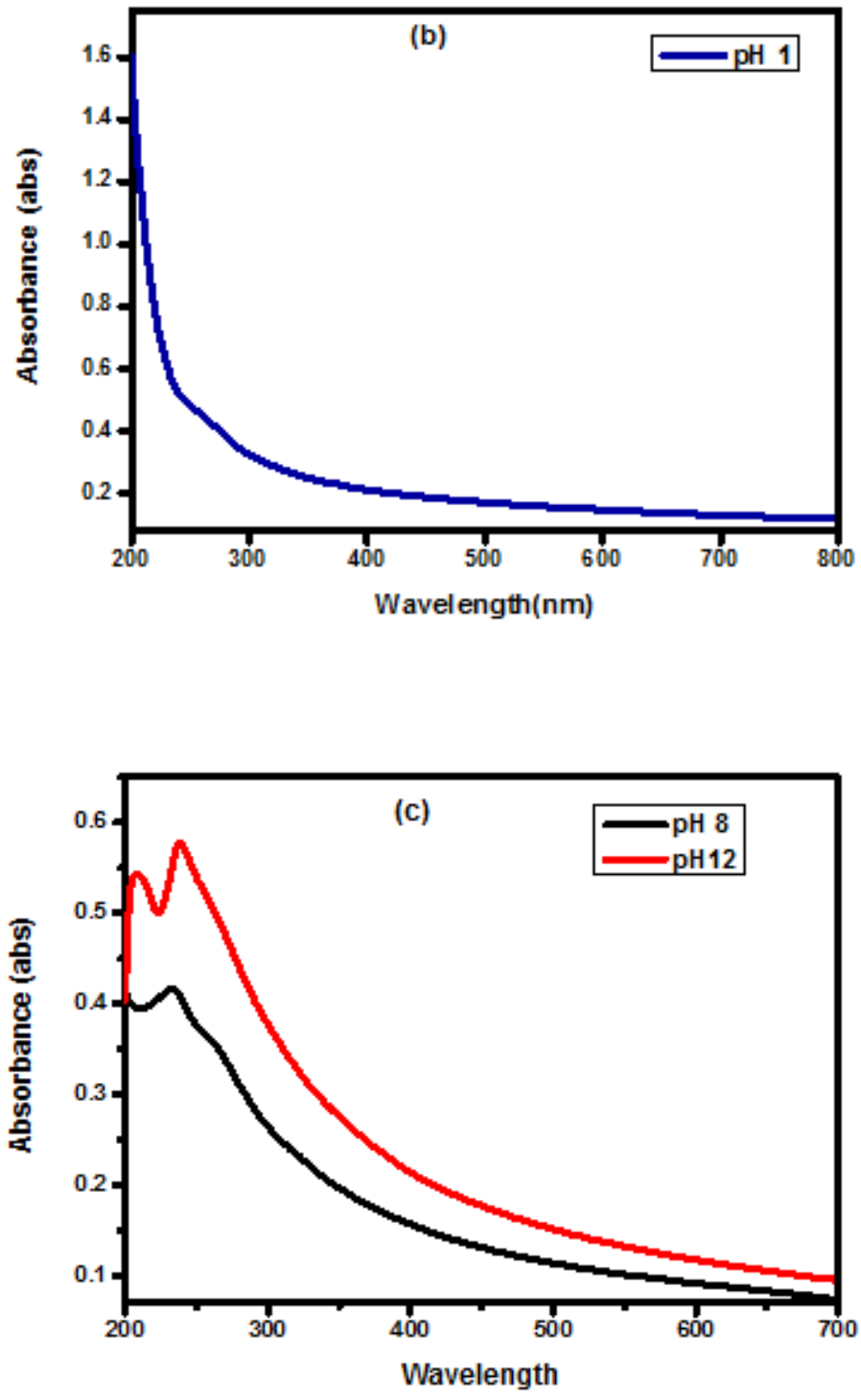

Fig 19: UV-Vis absorption spectrum of Graphene Oxide (GO) at (a) pH 8 (inset the GO powder dissolved in distilled water). (b) pH 1 and (c) pH 8 and pH 14.

There is a peak at ~ 232 nm indicating π-π* transition of C-C and C=C bonds in sp^2 hybrid regions [fig 19 (a)]. There is a shoulder at ~283nm which indicates the n-π* transition of the C=O bond in sp^3 hybrid regions [fig 19 (a)]. Except these two peaks there is no another

obvious band edge absorption spike found upto 700 nm. At highly acidic medium of pH 1 we see that the absorption spectrum is slightly different but still has a peak ~235nm [fig 19 (b)].While when we compare the absorption spectrum of GO at pH 8 and 14 we see no such difference [fig 19 (c)]. The reason for this varied behaviour of GO with different pH can be attributed to the edge carboxyl groups interaction with the basal planes. These edge carboxyl groups on GO sheets are simply viewed as tunable means which changes the hydrophilicity of GO in aqueous media at varying pH.

Due to the presence of absorption peak at 232 nm the energy bandgap of graphene oxide comes out to be 5.34 eV [fig 20]. This bandgap plays a key role in the fluorescence behaviour of GO. Thus, it is observed that compared to graphene which is gapless, GO contains bandgap between it's valence and conduction bands.

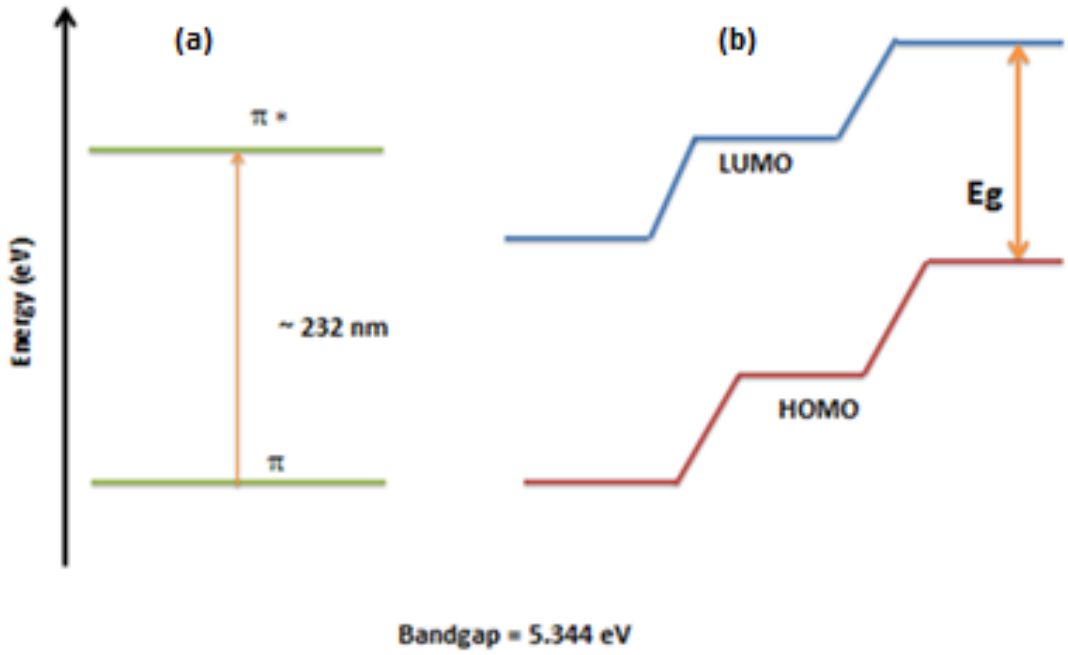

Fig 20: (a) π→π* transition at ~232 nm. (b) Energy level diagram of GO.

Due to absence of an energy bandgap in graphene,fluoroscence should not be possible in it unless assisted by phonons [52].However in contrast to graphene, GO has heterogeneous atomic and electronic structure which results in unexpected fluoroscence emissions in near infra-red,visible and ultra violet regions.

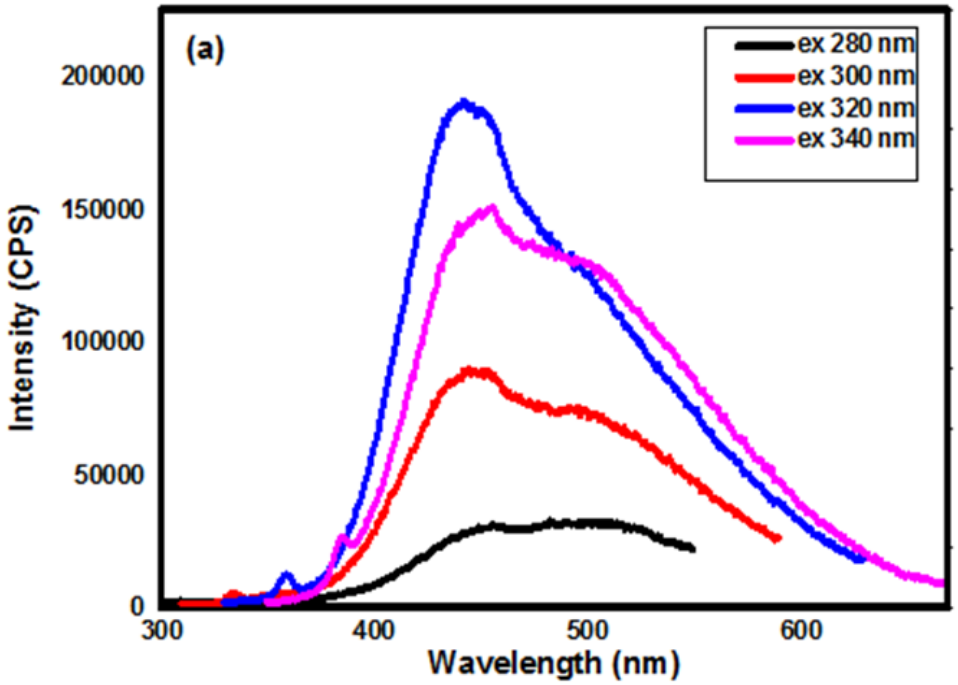
(a)
ex 280 nm
ex 300 nm
ex 320 nm
ex 340 nm
Intensity (CPS)
200000
150000
100000
50000
0
300
400
500
600
Wavelength (nm)

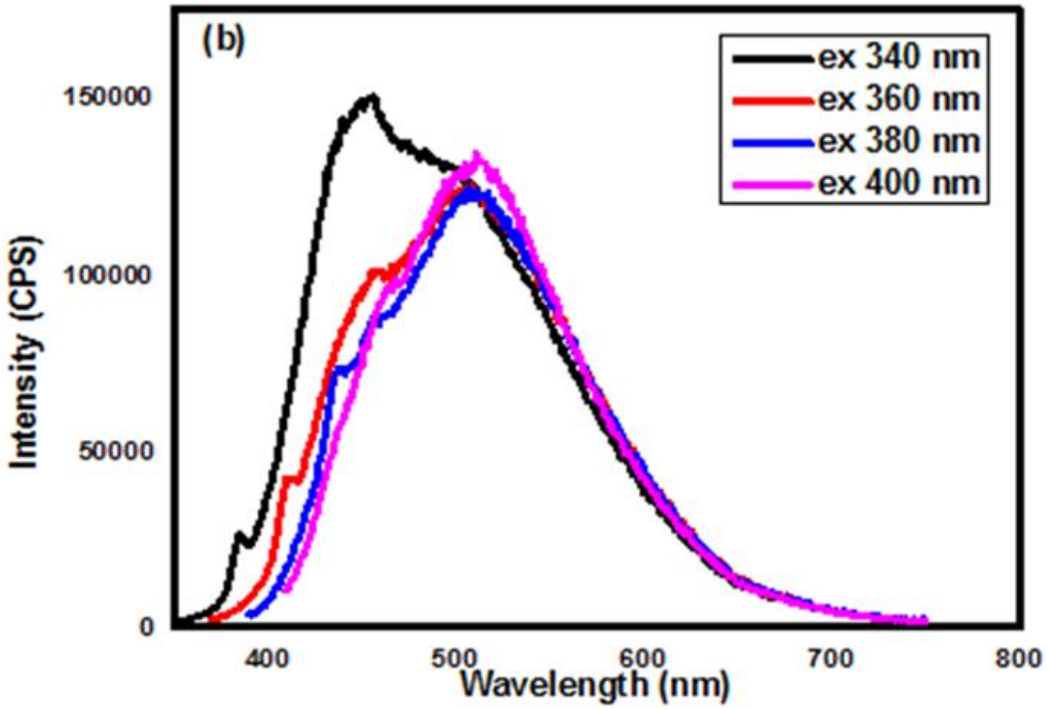
(b)
ex 340 nm
ex 360 nm
ex 380 nm
ex 400 nm
Intensity (CPS)
150000
100000
50000
0
400
500
600
700
800
Wavelength (nm)

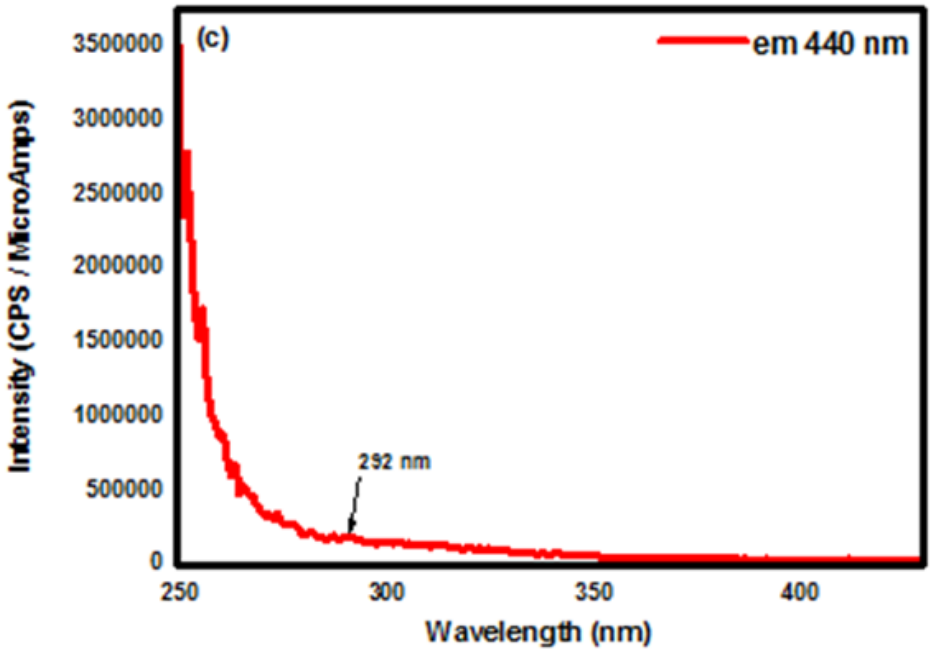

Fig 21 : Fluorescence spectra of GO with different excitation wavelengths ranging from (a) 280-340 nm. (b) 340-400 nm. (c) excitation spectrum of GO.

In the range of 280-340 nm one sharp peak ~ 443nm is observed. Also, the 320 nm excitation wavelength has the maximum intensity and peak at 443 nm [fig 21 (a)]. Also there is presence of another peak ~ 497-515 nm [fig 21 (a)]. These two peaks indicate the presence of both blue and green emissions. At higher excitation wavelengths from 340-400 nm it is observed that the first peak is vanishing whereas the second peak is becoming more prominent [fig 21 (b)]. In this spectra we have observed that there is no shifting in peaks as we move towards higher excitation wavelengths. Thus, the emission wavelength is independent of excitation wavelength in GO.Typically semiconductors show fluoroscence due to band edge transitions but due to the presence of strong heterogeneous atomic and electronic structure in GO the fluoroscence arises from electron-hole pairs in localized electronic states as a consequence of various possible configurations. It is generally taken into account the fluoroscence of GO varies depending on the mechanism undertaken for synthesizing them. Also this intrinsic and tunable fluoroscence of GO could open exciting new optical and electronics applications for graphene based systems.

The excitation spectrum of GO is taken with 440 nm emission wavelength. There is a presence of a small peak ~292 nm which is in accordance with $n \rightarrow \pi^*$ transition as observed from the absorption spectrum [fig 21 (c)].Other than this, no peak is observed.

The solid GO powder which was obtained by modified hummers method was directly used for X-ray diffraction without any further changes.

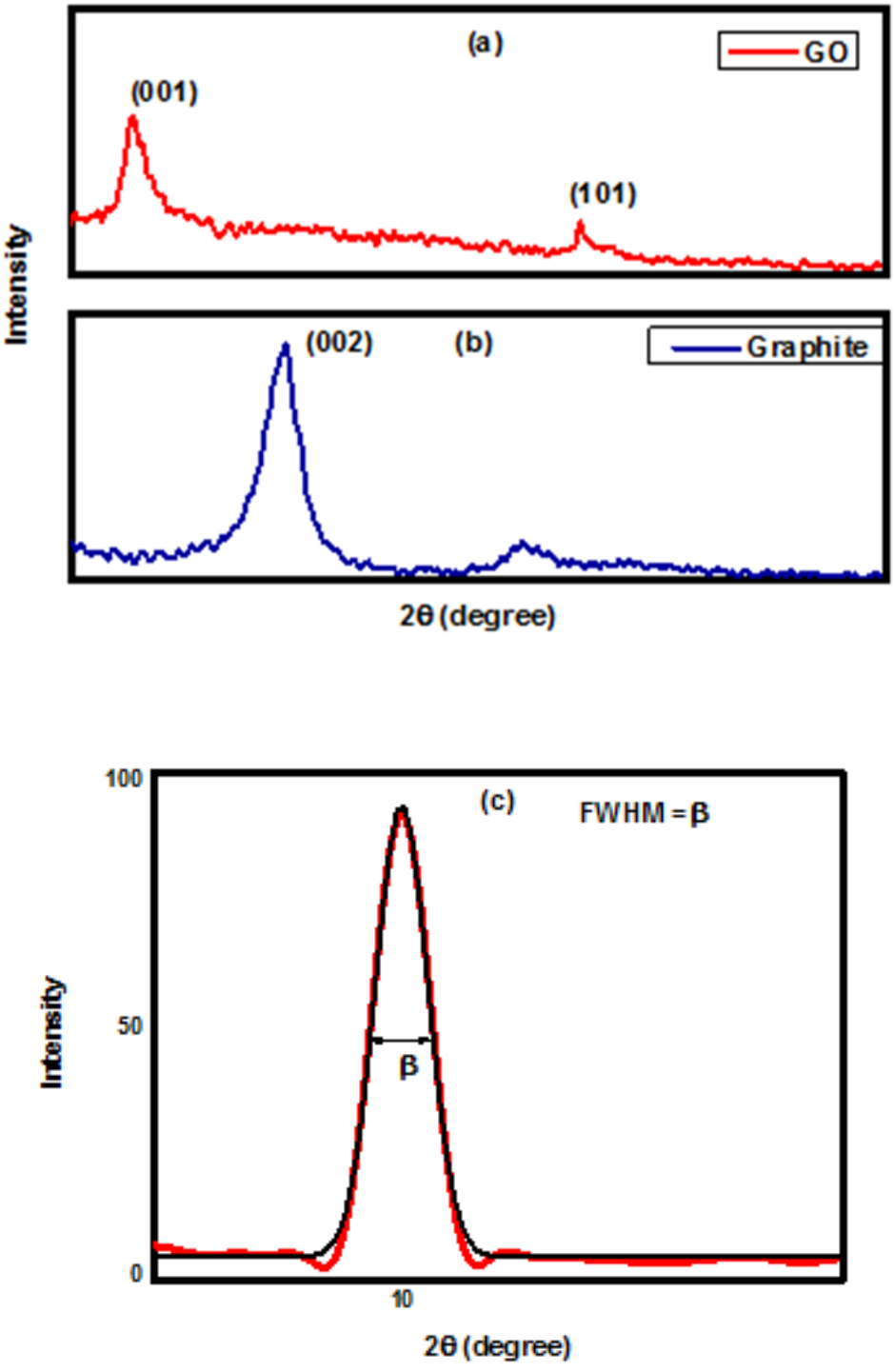

Fig 22: (a) XRD patterns of GO and graphite. (b) Calculated FWHM of GO.

An intense diffraction peak is observed for GO which is centered at 2Θ value of 10.01˚ or 0.087 radians corresponding to 8.815 A˚ inter layer spacing [fig 22 (a) and I]. There is also

one small peak at ~43˚ which is due to the traces of MnO_2 present in the sample [fig 21 (a)]. While for graphite the value of 2Θ is ~26.02˚ [fig 22 (b) and I].Thus, the inter layer spacing is calculated by the equation

$$d = \frac{\lambda}{2\sin\Theta} \text{ ---------- (7)}$$

Here d stands as the inter-stack separation, Θ is the half value of the corresponding angle of diffraction and λ is the X-ray source wavelength used. The calculated FWHM for GO comes out to be 0.556˚ [fig 22 (c) and I]. Compared to the base material graphite having d~3.34 A˚ [table 1], the inter layer spacing of graphene oxide is calculated to be more than double of it's value. Generation of oxygeneted polar functionalities over graphene layers is the main reason for the increase in the stack separation of GO compared to graphite. The as prepared GO is hydrophilic in nature resulting in the presence of some quantity of water molecules between the layers as entrapped species, thus also adding up to the d value [54]. To be precise, sp^3 defects and introduction of functional groups are the main reasons for the increase in the stack separation as the quantitative amount of water sub molecules present between the stacks are way lesser compared to them. Thus, their contribution to d value is very less.

The peak width of GO is mainly dependent on graphitic domain structures and their sizes which are present inside the macroscopic graphene materials. This observation is in contrast with the XRD peak positions as they depend on the inter-layer spacing. When we consider the separation of these graphitic domains we observe that in lateral direction they are separated by grain boundaries while in longitudinal direction by sp^2/sp^3 domain boundaries. The Debye-Scherer equation is widely used to determine the crystallite width of GO. The equation is given by

$$D = \frac{0.89\,\lambda}{\beta\cos\Theta} \text{ --------- (8)}$$

Where β represents the width of diffraction peak at half maximum height (FWHM) expressed in radians, Θ stands for the half diffraction angle of peak corresponding to inter layer spacing of GO in radians, while K is a constant which is related to the crystallite shape, normally taken as 0.89 for spherical crystals with cubic unit cells. Therefore, the crystallite width calculated for the as prepared GO comes out to be 141.843 A˚ [I]. There is one more parameter known as in-plane crystalline size which is determined considering the in-plane periodicity at 2Θ~43˚ shown as L.

$$L = \frac{1.84\lambda}{\beta\cos\Theta}.\text{----------(9)}$$

Therefore, the value of L~491.1 A˚ [I].Using both the above equation of Debye-Scherrer as well as Bragg's equation we can calculate the average number of graphene layers (N) per domain. Combining both equations we get

$$N = \frac{D}{d} + 1\text{----------(10)}$$

The value of n for GO comes out to be ~17 [I]. Thus, we can state that there are 17 number of graphene layers present per domain in GO.

Table I) Various physical parameters that are obtained by XRD of GO and graphite.

	2Θ (degree)	**FWHM(degree)**	**d (A˚)**	**D (A˚)**	**Number of layers (n)**	**L (A˚)**
GO	10.01	0.55576	8.815	141.843	17	491.1
Graphite	26.02	3.55359	3.34	8.2	3	258.0

As we know Fourier transform infrared spectroscopy is a technique which is based on the atomic and molecular vibrations of bonds present in a sample. This technique is used to obtain infrared spectrum of emission or absorption of a solid, liquid or gas. The sample for FT-IR characterization was obtained by diluting ~0.02 g of GO powder in 5 ml of distilled water.

A broad peak at 3338.20 cm^{-1} is observed which is because the medium was water and it indicates the presence of O-H stretching [fig 23 and II]. The peak obtained at 1634.45 cm^{-1} shows the presence of C=C bonds which results in $\pi \rightarrow \pi^*$ transition in GO [fig 23 and II]. The peak at 1365 cm^{-1} stands for C-O-H bonds which are generally confined in the sp^3 sites [fig 23 and II]. Also there is a peak of C-O at 1214 cm^{-1} which is due to the oxidation of graphite by strong acids [fig 23 and II]. Also the peaks from 555.59 cm^{-1} to 499 cm^{-1} indicates the finger print region of GO which are unique for every material [fig 23 and II]. Thus, the FT-IR spectrum of GO indicate the presence of the bonds and functional groups which get added on the graphite surface due to modified hummer's method.

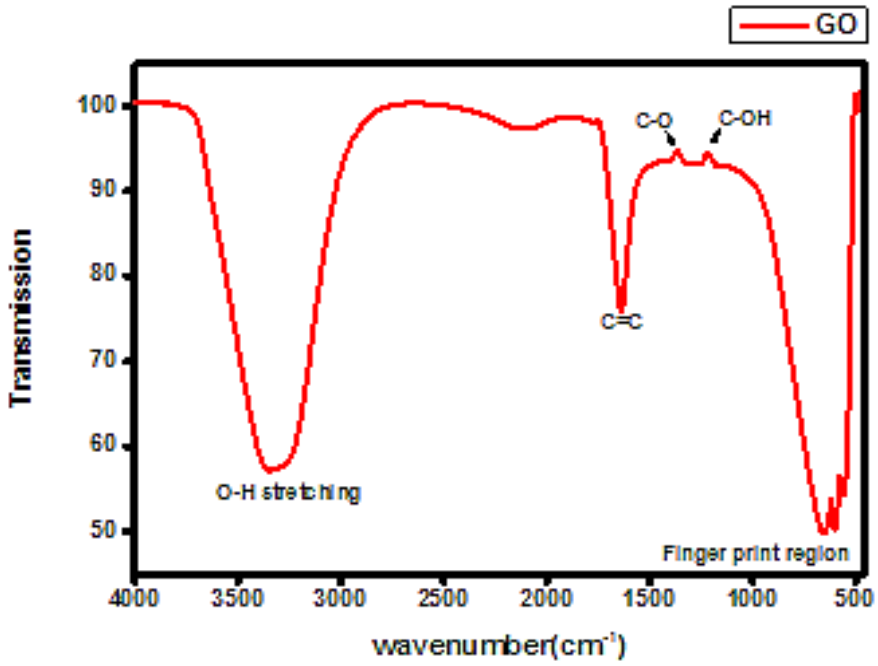

Fig 23 : FT-IR spectrum of GO.

Table II) Various functional groups and their frequency ranges that are obtained from FT-IR of GO.

S.No	**Frequency Range (cm^{-1})**	**Functional Group**
1.	3338.20	O-H Stretching
2.	1634.45	C=C
3.	1365	C-O-H
4.	1214	C-O
5.	555.59-499	Finger print region

The TEM characterization of the GO powder was perfomed with Technai F20 at 220 kV for different maginification values. The images indicate that sheets of GO are formed [fig 24 (a),(b),(c) and (d)]. These sheets are 100 nm in length. In the fig 24 (d) it is clearly observed that the sheet of GO are almost transparent. These sheets are also hydrophilic in nature as they get easily dissolve in distilled water.

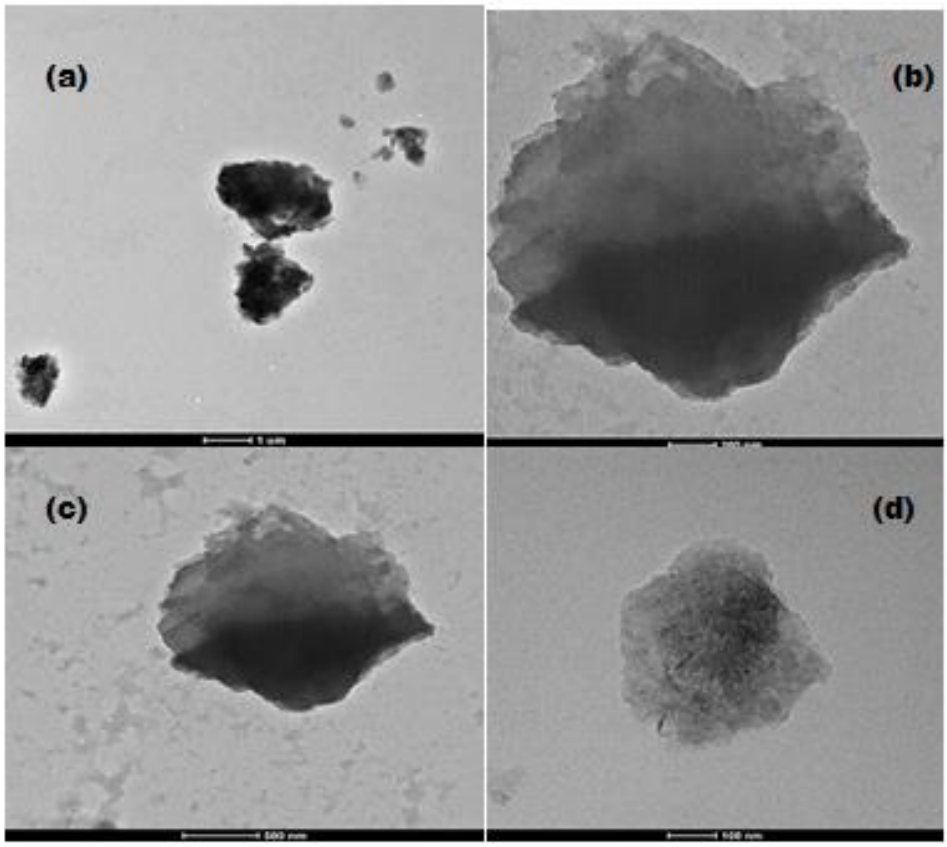

Fig 24 : TEM images of GO at magnifications of (a) 1um (b) 500 nm (c) 200 nm and (d) 100 nm.

4.2) Graphene quantum dots (GQDs).

The oxidative cutting of GO powder with strong acids result in the formation of GQDs which are pale yellow in colour. The various colour changes in the process of GQDs formation are shown below in fig 25.

Fig 25: The colour changes during GQDs formation process.

The sample of GQDs for various characterizations was prepared by taking 1 ml of GQDs stock solution in 2 ml of distilled water. The UV-Vis absorption spectrum of GQDs was measured by taking the as prepared sample in a 2mm cuvette.

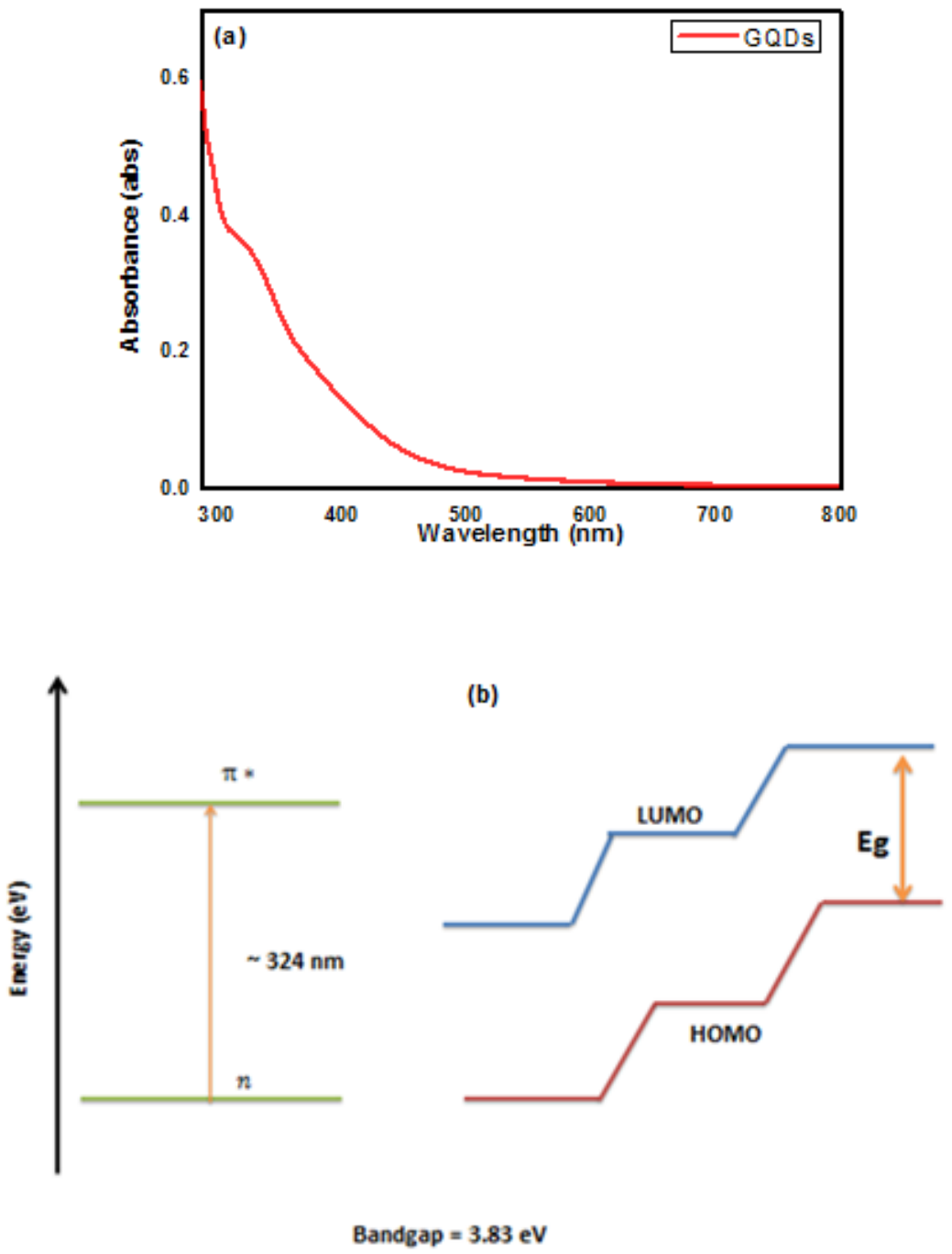

Fig 26: (a) shows the UV-Visible absorption spectrum of GQD. (b) Energy band diagram of GQDs.

A peak is observed ~ 324 nm indicating n→π* transition of C=O or other functional groups present on the surface [fig 26 (a)].It is generally observed that the preparation method of GQDs play a significant role towards it's various optical and electronic behaviours. The

defects combined with functional groups trapped in sp^3 sites of GQDs result in absorption peak around ~324 nm**.** The absorption peak of GQDs at ~324 nm leads to the presence of a bandgap having energy 3.83 eV [fig 26 (b)].Compared to GO we observe that the bandgap is decreasing as we are moving from two dimension to zero dimension. Thus, the conductivity of GQDs is more as compared to GO and therefore, they can be used for various optoelectronic applications.

PL in GQDs arises due to quantum confinement effect and surface states [57]. Carbon core present in GQDs result in quantum confinement effect. Surface states are due to the presence of functional groups present on the surface [57]. The FT-IR analysis suggest the presence of C−H, C−O,C=O, and O−C=O functional groups on the surface of GQDs. These groups significantly contribute to the luminescence of GQDs. As reported there are basically two major reasons for the photoluminescence of GQDs. GQDs have sp^2 sites in their structures therefore, the first reason is related to these sp^2 conjugation domains[52-60].Photoluminescence of GQDs arises due to emission from these sp^2 carbon backbone. Since these sp^2 domains are small enough due to quantum confinement effect, they have finite bandgap. This effect is usually known as size effect emission as the emission wavelength is determined by their sizes [57]. When synthesizing GQDs by using top-down approach these sp^2 domains tend to become heterogeneous and therefore excitation with a certain wavelength will selectively excite sp^2 sites depending on their size. It is popularly known as excitation dependent emission, and the origin of these emissions clearly depends on the varied conjugation lengths of the sp^2 hybrid carbon domains.

The second major reason for the photoluminescence of GQDs is the introduction of defects on their surface. These defects can be anything related to structural disruption of aromatic rings or simply because of the addition of functional groups during chemical oxidative synthesis of GQDs. Usually the second one is often considered as the main reason for the presence of defects in the GQDs structure. Generally these defects sites and sp^2 conjugated domains are independent of each other. Specially the defects are isolated and localized from other chromophores present. Due to such isolation these defects are usually treated as “molecular states” by many groups as they rather exist as individual molecules than been considered as components of the quantum confined structure. Thus, emission from defects predominantly depends on the structure of the localized sites, than size of the GQDs. It is recently observed that the pH changes have a very great impact on the defect emission of GQDs due to protonation or deprotonation of the functional groups.

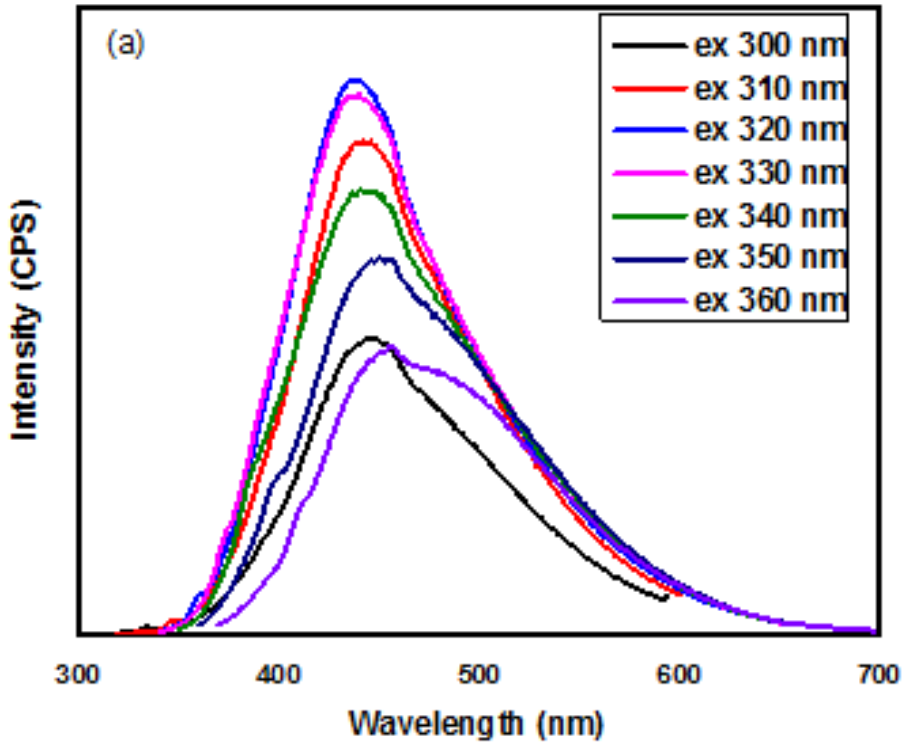
(a)
ex 300 nm
ex 310 nm
ex 320 nm
ex 330 nm
ex 340 nm
ex 350 nm
ex 360 nm
Intensity (CPS)
300
400
500
600
700
Wavelength (nm)

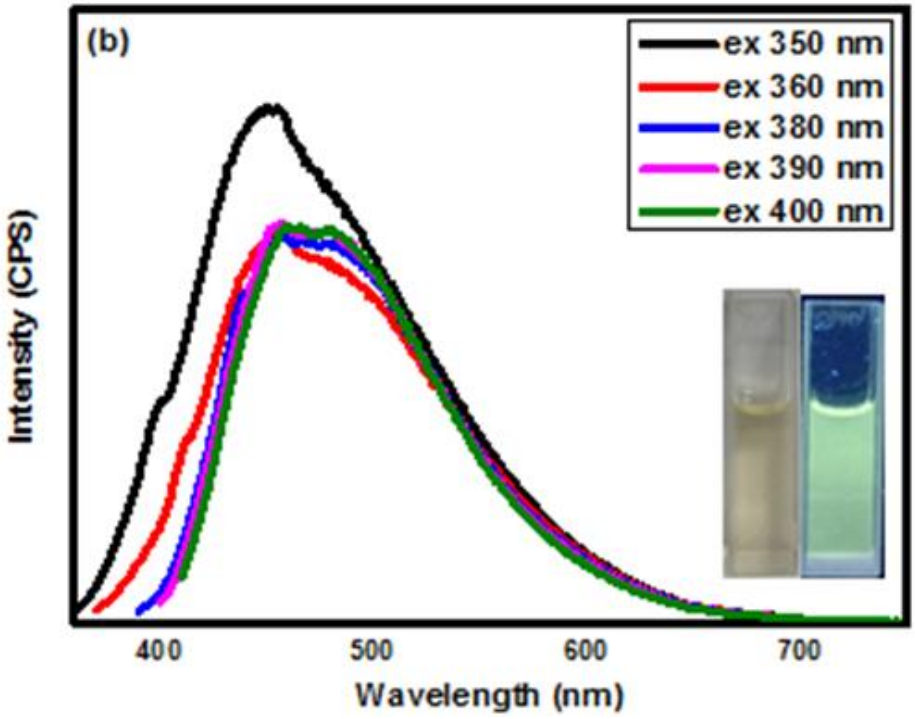
(b)
ex 350 nm
ex 360 nm
ex 380 nm
ex 390 nm
ex 400 nm
Intensity (CPS)
400
500
600
700
Wavelength (nm)

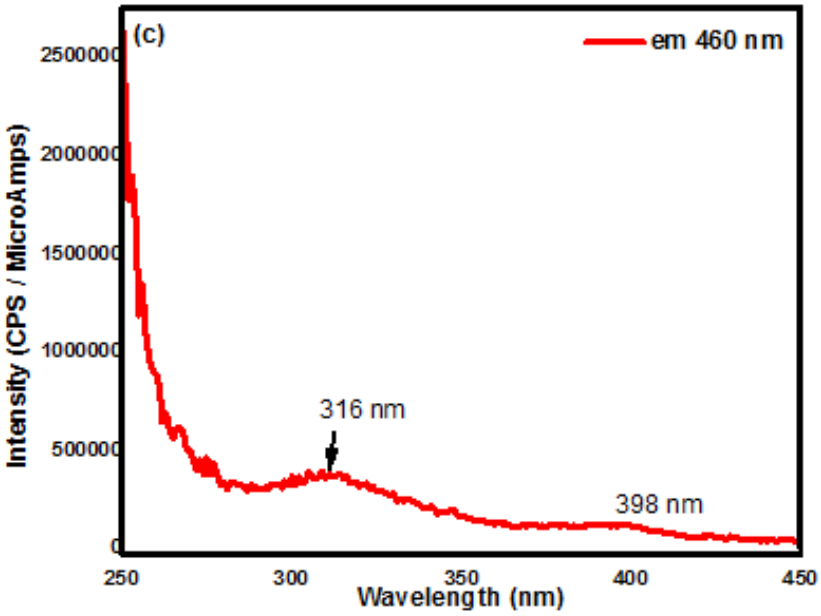

Fig 27: Emission spectra of GQDs with different excitation wavelengths ranging from (a) 300-360 nm.(b) 350-400 nm.(Inset : The colour variation of GQDs when exposed to normal light and UV light).(c)Excitation spectrum of GQDs with emission at 460 nm.

The emission spectra of GQDs with excitation wavelengths between 300-360 nm having increments of 10 nm shows one at ~ 440 nm [fig 27(a)].The 320nm excitation wavelength have the maximum intensity and peak at ~440 nm. Initially when the excitation wavelength is increasing from 300-320 nm the intensity of fluorescence also increases but as the excitation wavelength further increases from 320-360 nm the intensity decreases but the shifting in peak is very little. This indicates that the emission wavelength is independent of the excitation wavelength. But the value of emission peak intensity reduces with increase in excitation wavelength. Variation in excitation wavelength causes a change in intensity. This could be due to differently sized GQDs and surface states. The peak ~440 nm could possibly due to armchair or zig zag edges. But on further increase of the excitation wavelength from 350-400 nm we observe that the intensity of peak decreases [fig 27 (b)]. Thus,the intensity of the emission spectrum decreases with increase of excitation wavelength.

The excitation spectrum of GQDs was obtained at 440 nm emission wavelength[fig 27(c)].Here one peak is at ~316 nm which is in accordance with the absorption peak of GQDs of 324 nm indicating the presence of $n \rightarrow \pi^*$ transition which is due the presence of C=O and other functional groups. There is one another peak at ~ 398 nm which might be due to surface states and edge effects present in GQDs.

For observing the dependence of GQDs fluorescence on pH we have taken 1 ml GQDs stock solution in 2 ml distilled water and then varied the pH by diluting it with 0.1 M NaOH solution for different values as obtained from the automatic pH meter.

The GQDs in this experiment are synthesized by oxidative cutting of GO sheets by strong acids which results in the formation of many defects and trap sites on it's surface. It was earlier reported by Deng et al [58] that as the pH value increases, the number of trap sites present on the surface decreases. This reduction of trap sites improves the fluorescence efficiency and intensity of the as prepared GQDs . Not only intensity, it is also observed that with increasing pH the spectrum become narrower in width as well [fig 27(a) and (b)]. Thus, this phenomenon indicates that the pH value could significantly modify the fluorescence characteristics not just in intensity but also in wavelength. Thus, the above presented information evidences that the pH value is a very important factor which can be used to tune the optical properties of GQDs.

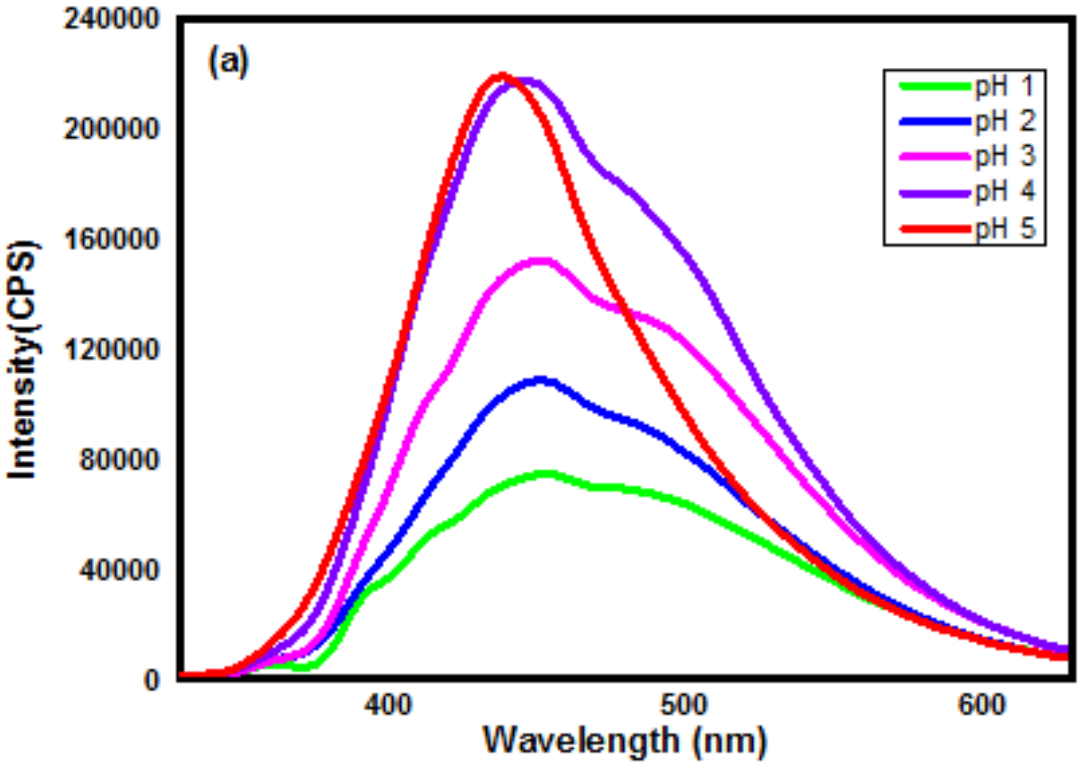

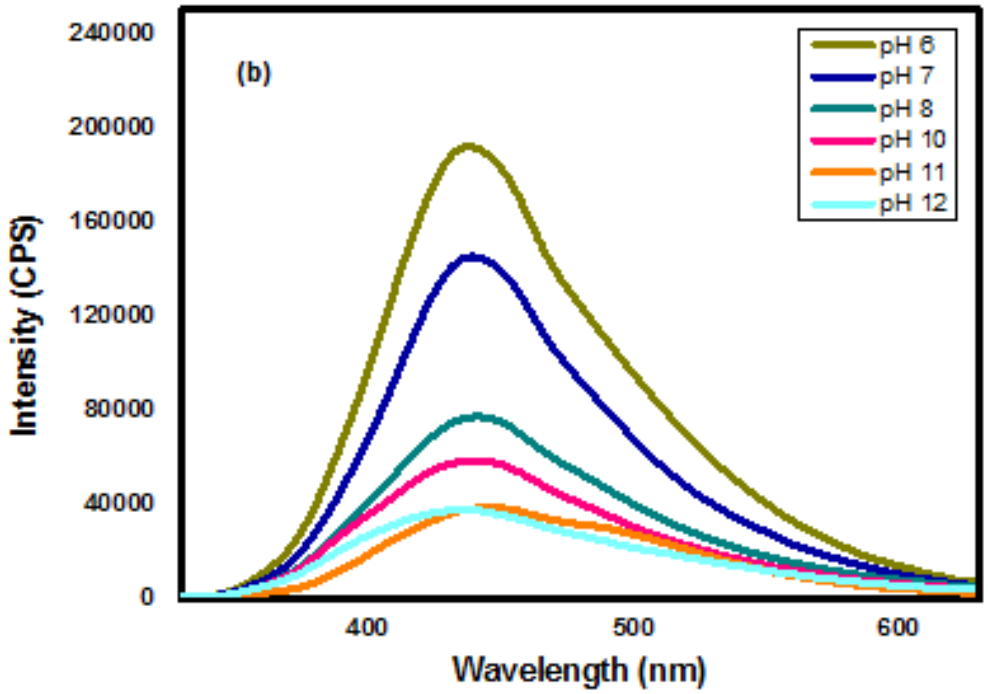

Fig 28: The fluorescence behaviour of GQDs at different pH values ranging from (a) 1-5. (b) 6-12.

From fig 28(a) and fig 28(b) we observed initially when the solution was extreme acidic between pH 1 to pH 4 there are two bands one ~ 443 nm and the other one ~ 487nm. Also the intensity keeps on increasing with the increasing value of pH in acidic medium. But as pH 5 is reached, we see that the spectrum shows only one sharp peak at ~442 nm. The prominence of the other peak which was present earlier vanishes. Now, as the medium shifts towards neutral we observe that the fluorescence spectrum of GQDs exhibit only one peak and there is no shifting but again,as the pH shifts from neutral to basic the intensity decreases. Thus, it is observed that the variations in pH changes the fluorescence intensity of the GQDs.

It is observed, not just the intensity but the fluorescence of the GQDs also narrows down the width of the spectrum with the increasing pH. We have also observed the variation of these different valued pH solutions of GQDs with different excitation wavelengths [fig 29 (a),(b) and (c)].

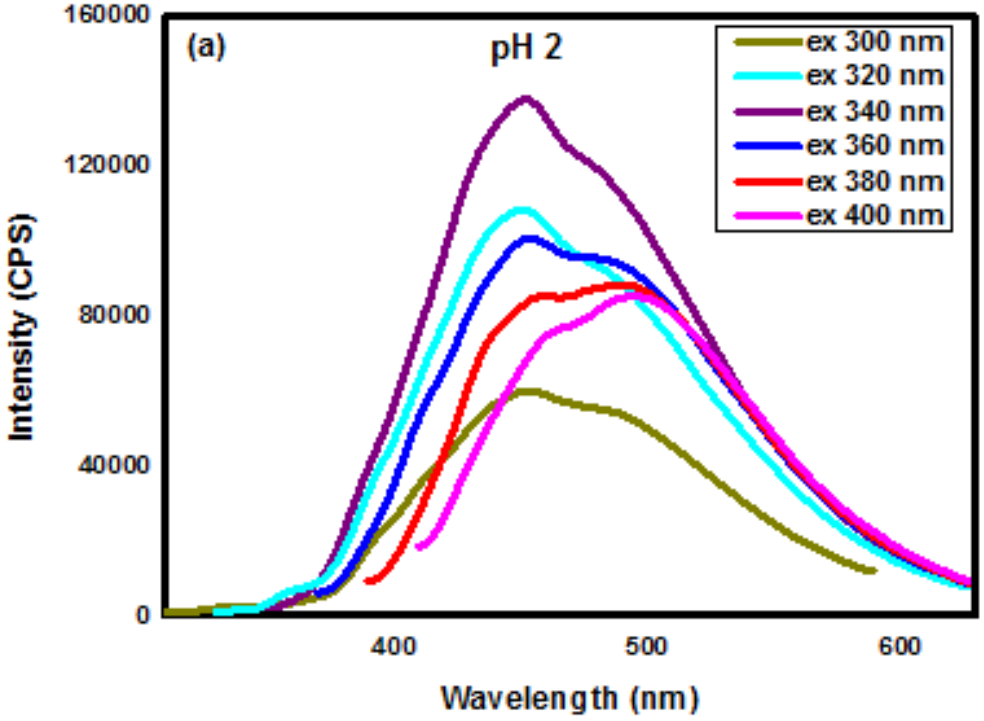
(a)
pH 2
ex 300 nm
ex 320 nm
ex 340 nm
ex 360 nm
ex 380 nm
ex 400 nm
Intensity (CPS)
160000
120000
80000
40000
0
400
500
600
Wavelength (nm)

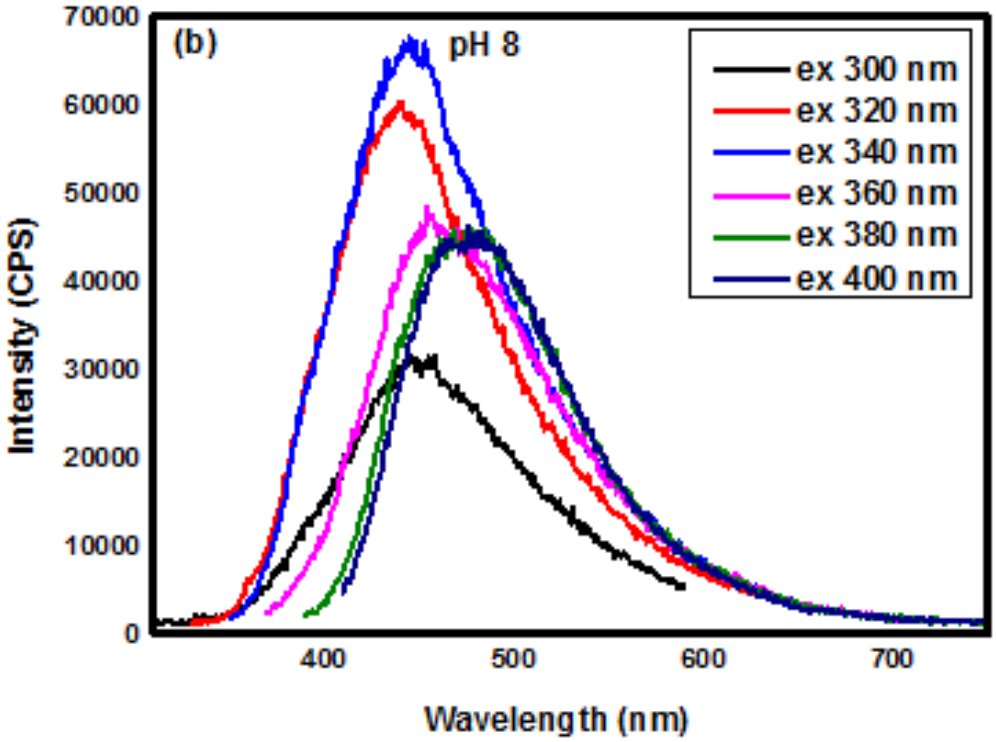
(b)
pH 8
ex 300 nm
ex 320 nm
ex 340 nm
ex 360 nm
ex 380 nm
ex 400 nm
Intensity (CPS)
70000
60000
50000
40000
30000
20000
10000
0
400
500
600
700
Wavelength (nm)

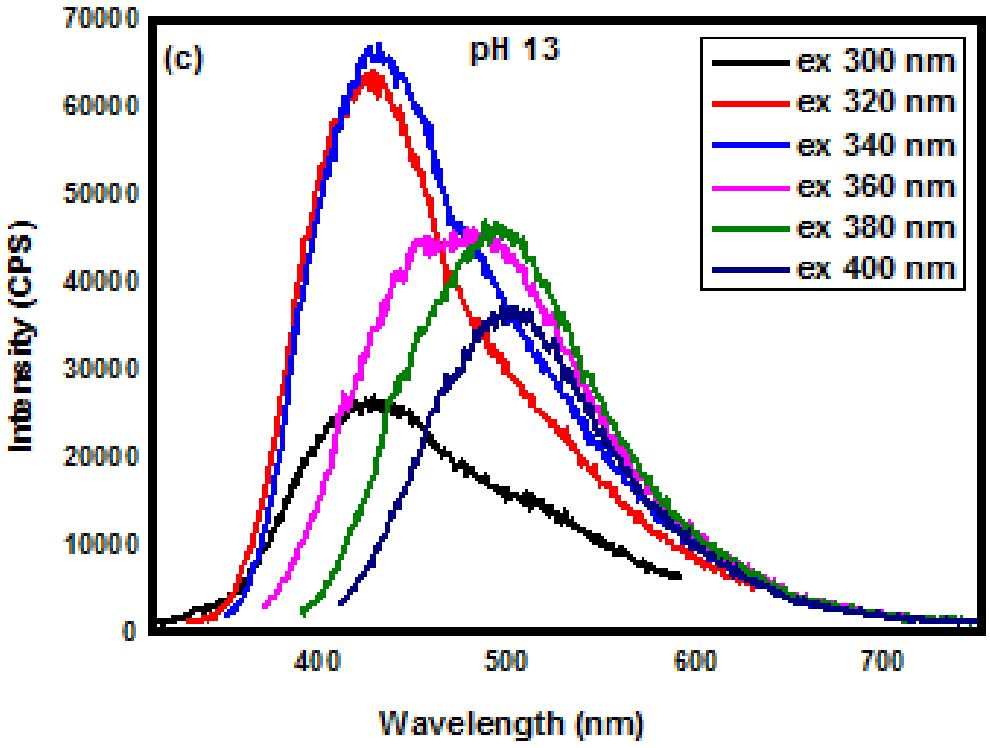

Fig 29: The emission spectra of GQDs for (a) pH 1 (b)pH 8 and (c)pH 13 at excitation wavelengths ranging from 300-400 nm.

Fig 29 shows emission spectra of GQDs at different pH with different excitation wavelengths ranging from 300 to 400 nm with increments of 20 nm. For the acidic environment at pH 1 we observe that the peaks are broad initially and also the intensities are increasing with the increase of excitation wavelengths from 300 to 340 nm. But with further increase of excitation wavelengths the intensity starts decreasing [fig 29 (a)]. The peak for excitation wavelength 340 nm has the maximum intensity. Initially, two peaks were observed at ~443 nm and the other at ~483 nm. But as the wavelength increases the peak shifts towards the longer wavelength and the signal has only one prominent peak with decrease in intensity. This in turn reveals that in acidic solution the fluorescence signal of GQDs is more favourable to shorter wavelength light. Compared to acidic medium the pH 8 spectrum of GQDs solution has narrower width with only one visible peak around ~445 nm [fig 29 (b)]. This behaviour is well explained above due to reduction of trap sites. But similar to acidic medium here also the 340 nm excitation wavelength has maximum intensity and the intensity further decreases with the increase of wavelength from 360-400 nm. Also there is shifting of peaks from blue emission region to green emission region. Whereas, at pH 13 the spectrum is little broader compared to pH 8 and but here also, only one peak is prominent [fig 29 (c)]. The shifting of signal towards longer wavelength with the increase of excitation wavelength

is more in the basic medium compared to when the solution was at pH 8. Thus, from all the information gathered above about the fluorescence spectrum of GQDs, it can be concluded that the spectrum not only depend upon the pH value of the solution but also on the excitation wavelength. Thus, these two can be used efficiently to tune the intensity and wavelength of GQDs for various optical applications as per the requirement.

As we know Fourier transform infrared spectrum is a widely used technique which helps us in determining various bonds present in a sample depending on the vibrational modes of the atoms when they are energized from low to higher energy levels.

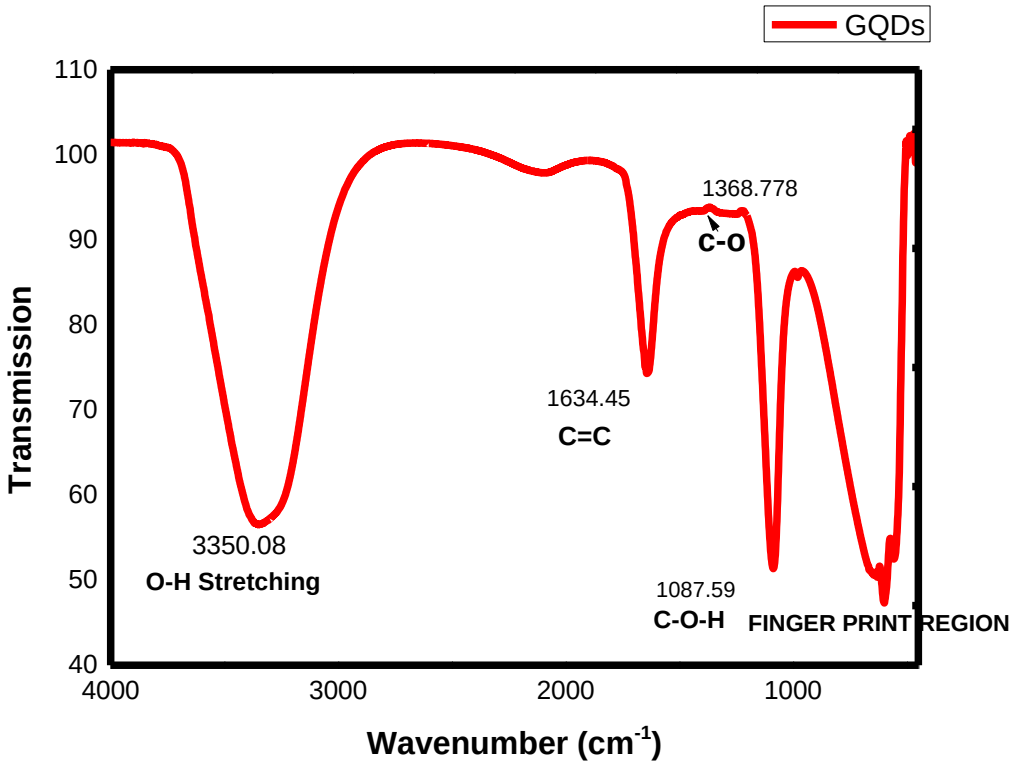

Fig 30: FT-IR spectrum of Graphene quantum dots (GQDs).

From fig 30 and III we observe a broad peak at 3350.08 cm^{-1} which is because the medium was water and it indicates the presence of O-H stretching. The peak obtained at 1634.45 cm^{-1} shows the presence of C=C bonds which results in $\pi \rightarrow \pi^*$ transition in GQDs. The peak at 1087.59 cm^{-1} stands for C-O-H bonds which are generally confined in the sp^3 sites. Also the peaks from 630 cm^{-1} to 460 cm^{-1} indicates the finger print region of GQDs which are unique for every material. Thus, the FT-IR spectrum of GQDs indicate the presence of the bonds and functional groups which are responsible for the peculiar behaviour of GQDs.

Table III) Various functional groups and their frequency ranges obtained from FT-IR of GQDs.

S.No	**Frequency Range**	**Functional Group**
1.	3350.08	O-H stretching
2.	1634.45	C=C
3.	1368.778	C-O
4.	1087.59	C-O-H
5.	630-460	Finger print region

CONCLUSION

After successfully synthesizing and evaluating the aim with which we started the experiment i.e. to do a comparative study between both the counterparts of wonder material graphene we can say that though graphene oxide is an insulator having bandgap ~5.344eV it shows fluoroscence due to the presence of the oxygenated functionalities present on it's surface. While as we perform it's reduction by oxidative cutting to produce graphene quantum dots we see that the conductivity increases as the bandgap tends to decrease ~3.83 eV. Both these materials are fluorescent but though the emission wavelength of GO is independent of excitation wavelength, the emission wavelength of GQDs can be tuned by changing either their excitation wavelength or the pH. On contrary to GO, the fluoroscence of GQDs are due to defects or trap sites present on their surfaces. Due to these properties GQDs can be widely used for optoelectronic applications. The FT-IR spectrum obtained of both GO and GQDs shows the presence of various functional groups and also gives us a picture of how the chemical structure of GO is changing on reducing to obtain GQDs. The XRD pattern of GO gives a sharp peak at ~10.01˚ which indicates the presence of GO with hkl index values of (001). There is also one minute peak at ~43˚ which are an indicator of MnO_2 traces as GO was synthesized by modified hummers method with $KMnO_4$ as the main oxidizing agent. We observe how the interlayer separation of GO is more than double of the parent graphite from which it was synthesized. The TEM images obtained from Technai at 220 kV indicates the formation of GO sheets which are ~100 nm in length. Thus, though the structural configuration of both GO and GQDs still need to explore more due to their varied properties which are getting reported everyday we have successfully synthesized and characterized both these new age material in this report.

REFERENCES

1. Wallace, P. R., “The band theory of graphite”, Physical Review 1947, 71 (9), 622-634.

2. Karu, A. E.; Beer, M.,” Pyrolytic Formation of Highly Crystalline Graphite Films”,Journal of Applied Physics 1966, 37 (5), 2179-2181.

3.Isett, L. C.; Blakely, J. M.,” Segregation isosteres for carbon at the (100) surface of nickel”, Surface Science 1976, 58 (2), 397-414.

4. Novoselov, K. S.; Geim, A. K.; Morozov, S. V.; Jiang, D.; Zhang, Y.; Dubonos, S. V.; Grigorieva, I. V.; Firsov, A.”Electric field effect in atomically thin carbon films”,Science 2004, 306 (5696), 666-9.

5.Wakabayashi K, Sasaki KI, Nakanishi T, Enoki T,”Electronic states of graphene nanoribbons”, Science and Technology of Advanced materials 2010,1468-6996.

6. D. R. Cooper, B. D’Anjou, N. Ghattamaneni, B. Harack, M. Hilke, A. Horth, et al., "Experimental review of graphene," ISRN Condensed Matter Physics 2012 vol. 5(3), 657-662.

7.A. K. Geim and K. S. Novoselov, "The rise of graphene," Nature Materials 2007, vol. 6, pp. 183-191.

8.A Theoretical Study of Graphene Oxide Chemical Structure- Haining Luo, university of Queensland,2011.

9.R. Raccichini, A. Varzi, S. Passerini, and B. Scrosati, "The role of graphene for electrochemical energy storage," Nature Materials 2015, vol. 14, pp. 271-279.

10. X. Huang, X. Qi, F. Boey, and H. Zhang, "Graphene-based composites," Chemical Society Reviews 2012, vol. 41, pp. 666-686.

11.O. C. Compton and S. T. Nguyen, "Graphene Oxide, Highly Reduced Graphene Oxide, and Graphene: Versatile Building Blocks for Carbon-Based Materials," ACS nano 2010, vol. 6, pp. 711-723.

12. S. Pei and H.-M. Cheng, "The reduction of graphene oxide," Carbon 2012, vol. 50, pp. 3210-3228.

13.W. S. Hummers and R. E. Offeman, "Preperation of Graphitic Oxide," Journal of the American Chemical Society 1958, vol. 80, pp. 1339-1339.

14.M.Batzill, "The surface science of graphene: Metal interfaces, CVD synthesis, nanoribbons, chemical modifications, and defects," Surface Science Reports 2012, vol. 67, pp. 83-115.

15. B. Hu, H. Ago, Y. Ito, K. Kawahara, M. Tsuji, E. Magome, et al., "Epitaxial growth of large-area single-layer graphene over Cu(111)/sapphire by atmospheric pressure CVD," Carbon 2012, vol. 50, pp. 57-65.

16. Z. Sun, Z. Liu, J. Li, G.-a. Tai, S.-P. Lau, and F. Yan, "Infrared Photodetectors Based on CVD Grown Graphene and PbS Quantum Dots with Ultrahigh Responsivity," Advanced Materials 2012, vol. 24, pp. 5878-5883.

17 B. N. Chandrashekar, B. Deng, A. S. Smitha, Y. Chen, C. Tan, H. Zhang, et al., "Roll-to-Roll Green Transfer of CVD Graphene onto Plastic for a Transparent and Flexible Triboelectric Nanogenerator," Advanced Materials 2015, vol. 27, pp. 5210-5216.

18. S. Hofmann, P. Braeuninger-Weimer, and R. S. Weatherup, "CVD-Enabled Graphene Manufacture and Technology," Journal of Physical Chemistry Letters 2016, vol. 6, pp. 2714-2721.

19 V. Miseikis, D. Convertino, N. Mishra, M. Gemmi, T. Mashoff, S. Heun, et al., "Rapid CVD growth of millimetre-sized single crystal graphene using a cold-wall reactor," 2d Materials 2015, vol. 2.

20 C. Mattevi, H. Kim, and M. Chhowalla, "A review of chemical vapour deposition of graphene on copper," Journal of Materials Chemistry 2011, vol. 21, pp. 3324-3334.

21.Kaniyoor, A.; Baby, T. T.; Ramaprabhu, S,". Graphene synthesis via hydrogen induced low temperature exfoliation of graphite oxide", Journal of Materials Chemistry 2010, 20 (39), 8467-8469.

22. Chen, J.; Yao, B.; Li, C.; Shi, G."An improved hummers method for eco friendly synthesis of graphene oxide", Carbon 2013, 64, 225-229.

23. Marcano, D. C.; Kosynkin, D. V.; Berlin, J. M.; Alexander, S.; Sun, Z.; Slesarev, A.; Alemany, L. B.; Lu, W.; Tour, J. M.,"Improved synthesis of graphene oxide", ACS Nano 2010, 4 (8), 4806-4814.

24. Chen, J.; Li, Y.; Huang, L.; Li, C.; Shi, G.," High-yield preparation of graphene oxide from small graphite flakes via an improved Hummers method with a simple purification process" Carbon 2015, 81, 826-834.

25. Hummers, W. S.; Offeman, R. E.,"preparation of graphitic oxide", Journal of the American Chemical Society 1958, 80 (6), 1339-1339.

26. Stankovich, S.; Dikin, D. A.; Piner, R. D.; Kohlhaas, K. A.; Kleinhammes, A.; Jia, Y.; Wu, Y.; Nguyen, S. T.; Ruoff, R. S.,"Synthesis of graphene nanosheets by chemical reduction", Carbon 2007, 45 (7), 1558-1565.

27. Ponomarenko, L. A.; Schedin, F.; Katsnelson, M. I.; Yang, R.; Hill, E. W.; Novoselov, K. S.; Geim, A. K., Chaotic Dirac billiard in graphene quantum dots", Science 2008, 320 (5874), 356-358.

28. Takagahara, T.; Takeda, K., “Theory of the quantum confinement effect on excitons in quantum dots of indirect-gap materials”,Physical Review 1992 B, 46 (23), 15578-15581.

29. Zhu, S.; Zhang, J.; Qiao, C.; Tang, S.; Li, Y.; Yuan, W.; Li, B.; Tian, L.; Liu, F.; Hu, R.; Gao, H.; Wei, H.; Zhang, H.; Sun, H.; Yang, B.,” Strongly green-photoluminescent graphene quantum dots for bioimaging applications”, Chemical Communications 2011, 47 (24), 6858-6860.

30. Chong, Y.; Ma, Y.; Shen, H.; Tu, X.; Zhou, X.; Xu, J.; Dai, J.; Fan, S.; Zhang, Z.,” The in vitro and in vivo toxicity of graphene quantum dots”. Biomaterials 2014,35 (19), 5041-5048.

31. Fuyuno, N.; Kozawa, D.; Miyauchi, Y.; Mouri, S.; Kitaura, R.; Shinohara, H.; Yasuda, T.; Komatsu, N.; Matsuda, K.,”Insight into the multiple quasi-molecular states in ethylenediamine reduced graphene nanodots “Advanced Optical Material 2014,2(10),983-989.

32. Tang, L.; Ji, R.; Cao, X.; Lin, J.; Jiang, H.; Li, X.; Teng, K. S.; Luk, C. M.; Zeng, S.; Hao, J.; Lau, S. P., “Deep ultraviolet photoluminescence of water-soluble self-passivated graphene quantum dots.” ACS Nano 2012, 6 (6), 5102-5110.

33. Yeh, T. F.; Huang, W. L.; Chung, C. J.; Chiang, I. T.; Chen, L. C.; Chang, H. Y.; Su, W. C.; Cheng, C.; Chen, S. J.; Teng, H.,” Elucidating Quantum Confinement in Graphene Oxide Dots Based on Excitation-Wavelength-Independent Photoluminescence”. Journal of Physical Chemistry Letters 2016, 7 (11), 2087-2092.

34. Das, S. K.; Liu, Y.; Yeom, S.; Kim, D. Y.; Richards, C. I., “Single-particle fluorescence intensity fluctuations of carbon nanodots.” Nano letters 2014, 14 (2), 620625.

35. Dong, Y.; Chen, C.; Zheng, X.; Gao, L.; Cui, Z.; Yang, H.; Guo, C.; Chi, Y.; Li, C. M., “One-step and high yield simultaneous preparation of single- and multi-layer graphene quantum dots from CX-72 carbon black“Journal of Materials Chemistry 2012,22 (18), 8764-8766.

36. Tetsuka, H.; Asahi, R.; Nagoya, A.; Okamoto, K.; Tajima, I.; Ohta, R.; Okamoto, A., “Optically Tunable Amino-Functionalized Graphene Quantum Dots “Advanced materials 2012, Vol 34(69),5333-5338.

37. S. Bae, H. Kim, Y. Lee, X. Xu, J.-S. Park, Y. Zheng, et al., "Roll-to-roll production of 30-inch graphene films for transparent electrodes," Nature Nanotechnology 2010, vol. 5, pp. 574-578.

38.T. Kobayashi, M. Bando, N. Kimura, K. Shimizu, K. Kadono, N. Umezu, et al., "Production of a 100-m-long high-quality graphene transparent conductive film by roll-to-roll chemical vapor deposition and transfer process," Applied Physics Letters 2013, vol. 104.

39. E. S. Polsen, D. Q. McNerny, B. Viswanath, S. W. Pattinson, and A. J. Hart, "High-speed roll-to-roll manufacturing of graphene using a concentric tube CVD reactor," Scientific Reports, vol. 5, May 21 2015. Materials 2012, 24 (39), 5333-5338.

40. W. S. Koh, C. H. Gan, W. K. Phua, Y. A. Akimov, and P. Bai, "The Potential of Graphene as an ITO Replacement in Organic Solar Cells: An Optical Perspective," Ieee Journal of Selected Topics in Quantum Electronics, vol. 20, Jan-Feb 2014.

41.W. Cai, R. D. Piner, F. J. Stadermann, S. Park, M. A. Shaibat, Y. Ishii, et al., "Synthesis and solidstate NMR structural characterization of (13)C-labeled graphite oxide," Science, vol. 321, pp. 18151817, Sep 26 2008.

42 T. Szabo, O. Berkesi, and I. Dekany, "DRIFT study of deuterium-exchanged graphite oxide," Carbon, vol. 43, pp. 3186-3189, Dec 2005. [34] B. C. Brodie, "On the atomic weight of graphite," Philosophical Transactions of the Royal Society of London, vol. 149, pp. 249-259, 1859.

43 Z. Luo, Y. Lu, L. A. Somers, and A. T. C. Johnson, "High Yield Preparation of Macroscopic Graphene Oxide Membranes," Journal of the American Chemical Society, vol. 131, pp. 898-906, Jan 28 2009.

44 R. Beams, L. G. Cancado, and L. Novotny, "Raman characterization of defects and dopants in graphene," Journal of Physics-Condensed Matter, vol. 27, Mar 4 2015.

45.B. Qiu, Y. Zhou, Y. Ma, X. Yang, W. Sheng, M. Xing, et al., "Facile synthesis of the Ti3+ selfdoped TiO2-graphene nanosheet composites with enhanced photocatalysis," Scientific reports, vol. 5, 2015.

46.A. Lerf, H. Y. He, M. Forster, and J. Klinowski, "Structure of graphite oxide revisited," Journal of Physical Chemistry B, vol. 102, pp. 4477-4482, Jun 4 1998.

47. T. Szabo, O. Berkesi, P. Forgo, K. Josepovits, Y. Sanakis, D. Petridis, et al., "Evolution of surface functional groups in a series of progressively oxidized graphite oxides," Chemistry of Materials, vol. 18, pp. 2740-2749, May 30 2006.

48.W.. Scholz and H. P. Boehm, "Graphite Oxide .6. Structure of Graphtite Oxide," Zeitschrift Fur Anorganische Und Allgemeine Chemie, vol. 369, pp. 327-&, 1969 1969.

49. D. R. Dreyer, A. D. Todd, and C. W. Bielawski, "Harnessing the chemistry of graphene oxide," Chemical Society Reviews, vol. 43, pp. 5288-5301, Aug 7 2014.

50. T. Nakajima and Y. Matsuo,"Formation process and structure of graphene oxide," Carbon, vol. 32, pp. 469-475, 1994 1994.

51. Duosi Tang, Jingjing Liu, Xiaomei Yan, and Longtian Kang* ,"The graphene oxide derived graphene quantum dots with different photoluminescence properties and peroxidase-like catalytic activity "RSC,May(2016).

52. Jingzhi Shang, Lin Ma, Jiewei Li,Wei Ai,Ting Yu & Gagik G. Gurzadyan,"The Origin of Fluorescence from Graphene Oxide". Scientific Reports (2009).

53. Kian Ping Loh, Qiaoliang Bao, Goki eda and manish chhowalla,"Graphene oxide as a chemically tunable platform for optical applications" nature chemistry (2010).

54.Rahul Sharma, Neekanshika Chadha & Parveen Saini,'' Determination of defect density, Crystallite size and number of graphene layers in graphene analogues using X-ray diffraction and Raman spectroscopy'.Indian journal of pure & Applied Physics. Vol. 55,pp-625-629,2017.

55. Sung Kim,, Sung Won Hwang, Min-Kook Kim, Dong Yeol Shin, Dong Hee Shin, Chang Oh Kim, Seung Bum Yang Jae Hee Park, Euyheon Hwang, Suk-Ho Choi, Geunwoo Ko, Sunghyun Sim, Cheolsoo Sone, Hyoung Joon Choi, Sukang Bae, and Byung Hee Hong," Anomalous Behaviors of Visible Luminescence from Graphene Quantum Dots: Interplay between Size and Shape",ACS Nano, vol 6(9),8203-8208,2012.

56. M. A. Velasco-Soto, S. A. Pérez-García, J. Alvarez-Quintana, Yu-Cao, L. Nyborg and L. LiceaJiménez,"Selective band gap manipulation of graphene oxide by its reduction with mild reagents", Carbon, vol 93,967-973,2015.

57. Satyaprakash Ahirwar, Sudhanshu Mallick, and Dhirendra Bahadur,"Electrochemical Method To Prepare Graphene Quantum Dots and Graphene Oxide Quantum Dots". ACS Omega,2,8343-8353,2017.

58. Ch. Li, J. Zhang , Q. Xiong , G. Lorenzini , and Y. Yue,"The pH Effect on Thermal Response of Fluorescence Spectroscopy of Graphene Quantum Dots for Nanoscale Thermal Characterization",journal of engineering thermophysics, vol 27(3), 345-356,2018.

59."Photoluminescence mechanism and applications of graphene Quantum dots" ,Yiyang Liu, Doctoral dissertation, University of Kentucky(2017).

60. Kyle A.Ritter and Joseph W.Lyding,"The influence of edge structure on the electronic properties of graphene quantum dots and nanoribbons". Nature materials,vol 8(3),235-242, (2009).